AD-750 746

RESEARCH AND DEVELOPMENT OF RARE EARTH-TRANSITION METAL ALLOYS AS PERMANENT-MAGNET MATERIALS

Alden E. Ray, et al

Dayton University

Prepared for:

Air Force Materials Laboratory

August 1972

AFML-TR-72-202

Form Approved
Budget Bureau No. 22-R0293

RESEARCH AND DEVELOPMENT OF RARE EARTH-TRANSITION METAL ALLOYS AS PERMANENT-MAGNET MATERIALS

A. E. Ray and K. J. Strnat
Research Institute
University of Dayton

Sponsored by
Advanced Research Projects Agency
ARPA Order No. 1617

TECHNICAL REPORT AFML-TR-72-202
August 1972

Approved for public release; distribution unlimited.

The views and conclusions contained in this document are those of the authors and should not be interpreted as necessarily representing the official policies, either expressed or implied, of the Advanced Research Projects Agency or the U.S. Government.

Air Force Materials Laboratory
Air Force Systems Command
Wright-Patterson Air Force Base, Ohio

NOTICE

When Government drawings, specifications, or other data are used for any purpose other than in connection with a definitely related Government procurement operation, the United States Government thereby incurs no responsibility nor any obligation whatsoever; and the fact that the Government may have formulated, furnished, or in any way supplied the said drawings, specifications, or other data, is not to be regarded by implication or otherwise as in any manner licensing the holder or any other person or corporation, or conveying any rights or permission to manufacture, use, or sell any patented invention that may in any way be related thereto.

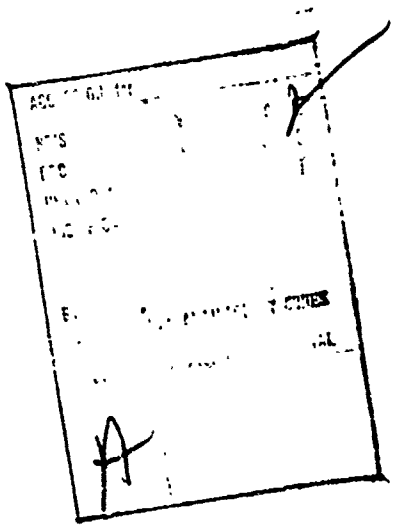

Copies of this report should not be returned unless return is required by security considerations, contractual obligations, or notice on a specific document.

Unclassified
Security Classification

DOCUMENT CONTROL DATA - R&D

(Security classification of title, body of abstract and indexing annotation must be entered when the overall report is classified)

1. ORIGINATING ACTIVITY (Corporate author)	2a. REPORT SECURITY CLASSIFICATION
University of Dayton Research Institute Dayton, Ohio 45469	Unclassified
	2b GROUP

3. REPORT TITLE

RESEARCH AND DEVELOPMENT OF RARE EARTH-TRANSITION METAL ALLOYS AS PERMANENT-MAGNET MATERIALS

4. DESCRIPTIVE NOTES (Type of report and inclusive dates)

Semiannual Interim Technical Report: 1 January 1972 - 30 June 1972

5. AUTHOR(S) (Last name, first name, initial)

Ray, Alden E.
Strnat, Karl J.

6. REPORT DATE	7a. TOTAL NO. OF PAGES	7b. NO. OF REFS
August 1972	67	25

8a. CONTRACT OR GRANT NO.	9a. ORIGINATOR'S REPORT NUMBER(S)
F33615-70-C-1625 b. PROJECT NO. 7371 c. Task No. 737103 d.	UDRI-TR-72-41
	9b. OTHER REPORT NO(S) (Any other numbers that may be assigned this report) AFML-TR-72-202

10. AVAILABILITY/LIMITATION NOTICES

Approved for public release; distribution unlimited.

11. SUPPLEMENTARY NOTES	12. SPONSORING MILITARY ACTIVITY
Details of illustrations in this document may be better studied on microfiche	Air Force Materials Laboratory Wright-Patterson AFB, Ohio 45433

13 ABSTRACT The results of thermomagnetic analyses of the $R_2(Co_{1-x}Fe_x)_{17}$ phases with R = Ce, Pr, Sm, Y, and MM above room temperature are reported, as well as the results of room temperature saturation magnetization for the phases with R = Ce, Pr, Nd, Sm, and Y. The magnetic transitions observed above the Curie points of the more iron-rich 2-17 phases in the alloys with R = Ce, Sm, and MM are believed due to the instability of the ternary phases in certain temperature and composition ranges. The room temperature saturation rises with increasing iron content throughout the easy c-axis composition ranges. The magnitude of the magnetocrystalline anisotropy has been measured on a large number of magnetically aligned powder specimens for the ternary phases with R = Ce, Pr, Sm, Y, and MM. The largest anisotropy is found in the system with R = Sm.

The phase $Ce_2(Co_{0.5}Fe_{0.5})_{17}$ has been re-examined by metallographic, x-ray diffraction, and electron microprobe analyses to explain the unusual thermal and magnetic transitions observed by DTA and TMA for the iron-rich $Ce_2(Co_{1-x}Fe_x)_{17}$ phases with $0.4 \leq x \leq 0.7$. The results indicate that $Ce(Co_{0.5}Fe_{0.5})_{17}$ is metastable at and near room temperature, and if heated to about 500°C, will spontaneously decompose into an iron-rich Co-Fe alloy (63at.% Fe) and a cobalt-rich $Ce_2(Co_{0.74}Fe_{0.26})_7$ phase.

The neodymium-cobalt alloy system has been re-examined and a revised phase diagram is proposed. Eutectics were found at 20 and at 36 at.% Co (625°C and 566°C, respectively). The following intermetallic phases were observed: Nd_3Co, Nd_xCo (29 at.% Co), $Nd_2Co_{1.7}$, Nd_2Co_3, $NdCo_2$, $NdCo_3$, Nd_2Co_7, Nd_5Co_{19}, $NdCo_5$ and Nd_2Co_{17}.

The results of some preliminary sintering experiments usind $NdCo_5$ and $DiCo_5$ as base metals and 60 Sm/40 Co and 70 Pr/30 Co alloys as sintering aids are reported. Intrinsic coercive forces of 4000 Oe and 8820 Oe were obtained with the 70 Pr/30 Co sintering aid for $NdCo_5$ and $DiCo_5$, respectively. A peak coercive force of 10280 Oe was obtained for $DiCo_5$ sintered with 60 Sm/40 Co.

DD FORM 1 JAN 64 1473

IR

Unclassified
Security Classification

14 KEY WORDS	LINK A		LINK B		LINK C	
	ROLE	WT	ROLE	WT	ROLE	WT
Magnetic Materials Magnetic Properties Permanent Magnets Rare Earth Alloys Intermetallic Compounds						

INSTRUCTIONS

1. ORIGINATING ACTIVITY: Enter the name and address of the contractor, subcontractor, grantee, Department of Defense activity or other organization *(corporate author)* issuing the report.

2a. REPORT SECURITY CLASSIFICATION: Enter the overall security classification of the report. Indicate whether "Restricted Data" is included. Marking is to be in accordance with appropriate security regulations.

2b. GROUP: Automatic downgrading is specified in DoD Directive 5200.10 and Armed Forces Industrial Manual. Enter the group number. Also, when applicable, show that optional markings have been used for Group 3 and Group 4 as authorized.

3. REPORT TITLE: Enter the complete report title in all capital letters. Titles in all cases should be unclassified. If a meaningful title cannot be selected without classification, show title classification in all capitals in parenthesis immediately following the title.

4. DESCRIPTIVE NOTES: If appropriate, enter the type of report, e.g., interim, progress, summary, annual, or final. Give the inclusive dates when a specific reporting period is covered.

5. AUTHOR(S): Enter the name(s) of author(s) as shown on or in the report. Enter last name, first name, middle initial. If military, show rank and branch of service. The name of the principal author is an absolute minimum requirement.

6. REPORT DATE: Enter the date of the report as day, month, year; or month, year. If more than one date appears on the report, use date of publication.

7a. TOTAL NUMBER OF PAGES: The total page count should follow normal pagination procedures, i.e., enter the number of pages containing information.

7b. NUMBER OF REFERENCES: Enter the total number of references cited in the report.

8a. CONTRACT OR GRANT NUMBER: If appropriate, enter the applicable number of the contract or grant under which the report was written.

8b, 8c, & 8d. PROJECT NUMBER: Enter the appropriate military department identification, such as project number, subproject number, system numbers, task number, etc.

9a. ORIGINATOR'S REPORT NUMBER(S): Enter the official report number by which the document will be identified and controlled by the originating activity. This number must be unique to this report.

9b. OTHER REPORT NUMBER(S): If the report has been assigned any other report numbers *(either by the originator or by the sponsor)*, also enter this number(s).

10. AVAILABILITY/LIMITATION NOTICES: Enter any limitations on further dissemination of the report, other than those imposed by security classification, using standard statements such as:

(1) "Qualified requesters may obtain copies of this report from DDC."

(2) "Foreign announcement and dissemination of this report by DDC is not authorized."

(3) "U. S. Government agencies may obtain copies of this report directly from DDC. Other qualified DDC users shall request through _____."

(4) "U. S. military agencies may obtain copies of this report directly from DDC. Other qualified users shall request through _____."

(5) "All distribution of this report is controlled. Qualified DDC users shall request through _____."

If the report has been furnished to the Office of Technical Services, Department of Commerce, for sale to the public, indicate this fact and enter the price, if known.

11. SUPPLEMENTARY NOTES: Use for additional explanatory notes.

12. SPONSORING MILITARY ACTIVITY: Enter the name of the departmental project office or laboratory sponsoring *(paying for)* the research and development. Include address.

13. ABSTRACT: Enter an abstract giving a brief and factual summary of the document indicative of the report, even though it may also appear elsewhere in the body of the technical report. If additional space is required, a continuation sheet shall be attached.

It is highly desirable that the abstract of classified reports be unclassified. Each paragraph of the abstract shall end with an indication of the military security classification of the information in the paragraph, represented as *(TS)*. *(S)*. *(C)* or *(U)*

There is no limitation on the length of the abstract. However, the suggested length is from 150 to 225 words.

14. KEY WORDS: Key words are technically meaningful terms or short phrases that characterize a report and may be used as index entries for cataloging the report. Key words must be selected so that no security classification is required. Identifiers, such as equipment model designation, trade name, military project code name, geographic location, may be used as key words but will be followed by an indication of technical context. The assignment of links, rules, and weights is optional.

I b

RESEARCH AND DEVELOPMENT OF RARE EARTH-TRANSITION METAL ALLOYS AS PERMANENT-MAGNET MATERIALS

By:

Dr. Alden E. Ray and Dr. Karl J. Strnat, Principal Investigators
University of Dayton, Research Institute and Electrical Engineering Dept.
300 College Park Ave., Dayton, Ohio 45469
Tel. Numbers (513) 229-3527 and (513) 229-3535

Sponsored by:

Advanced Research Projects Agency
ARPA Order No. 1617

Program Code No. OD10
Contract effective date: 30 June 1970
Expiration date: 30 June 1973
Amount of contract: $525,012

Submitted to:

Air Force Materials Laboratory, AFSC, USAF
Project Scientist: Mr. Donald J. Evans, LPE Tel. (513) 255-4474

IC

FOREWORD

The research described in this report is part of the contractual research program of the Materials Physics Division, Air Force Materials Laboratory. It was performed by the authors at the University of Dayton, Dayton, Ohio 45409, and was sponsored by the Advanced Research Projects Agency, ARPA Order No. 1617, Program Code No. OD10. The contract is administered under Project No. 7371, Task No. 737103, by the Air Force Materials Laboratory, Air Force Systems Command, Wright-Patterson Air Force Base, Ohio. The work was performed under contract F33615-70-C-1625, project scientist, Mr. Donald Evans (AFML/LPE/513-255-4474).

The participants in this research were Adolf Biermann, John Geis, Richard Harmer, Michael Hartings, Andrew Kraus, Robert Leasure, Herbert Mildrum, Shukdoor Rashidi, Alden Ray, Jacques Schweizer, Charles Shanley, Karl Strnat, Joseph Tront, James Tsui, and David Walsh.

This report covers research conducted between 1 January 1972 and 30 June 1972. The report was submitted by the authors in August 1972.

Publication of this report does not constitute Air Force approval of the report's findings and conclusions. It is published only for the exchange and stimulation of ideas.

Charles E Ehrenfried

CHARLES E. EHRENFRIED
Major, USAF
Chief, Electromagnetic Materials Br.
Materials Physics Division
Air Force Materials Laboratory

ABSTRACT

The results of thermomagnetic analyses of the $R_2(Co_{1-x}Fe_x)_{17}$ phases with R = Ce, Pr, Sm, Y, and MM above room temperature are reported, as well as the results of room temperature saturation magnetization for the phases with R = Ce, Pr, Nd, Sm, and Y. The magnetic transitions observed above the Curie points of the more iron-rich 2-17 phases in the alloys with R = Ce, Sm, and MM are believed due to the instability of the ternary phases in certain temperature and composition ranges. The room temperature saturation rises with increasing iron content throughout the easy c-axis composition ranges. The magnitude of the magnetocrystalline anisotropy has been measured on a large number of magnetically aligned powder specimens for the ternary phases with R = Ce, Pr, Sm, Y, and MM. The largest anisotropy is found in the system with R = Sm.

The phase $Ce_2(Co_{0.5}Fe_{0.5})_{17}$ has been re-examined by metallographic, x-ray diffraction, and electron microprobe analyses to explain the unusual thermal and magnetic transitions observed by DTA and TMA for the iron-rich $Ce_2(Co_{1-x}Fe_x)_{17}$ phases with $0.4 \leq x \leq 0.7$. The results indicate that $Ce(Co_{0.5}Fe_{0.5})_{17}$ is metastable at and near room temperature, and if heated to about 500°C, will spontaneously decompose into an iron-rich Co-Fe alloy (63 at.% Fe) and a cobalt-rich $Ce_2(Co_{0.74}Fe_{0.26})_7$ phase.

The neodymium-cobalt alloy system has been re-examined and a revised phase diagram is proposed. Eutectics were found at 20 and at 36 at.% Co (625°C and 566°C, respectively). The following intermetallic phases were observed: Nd_3Co, Nd_xCo (29 at.% Co), $Nd_2Co_{1.7}$, Nd_2Co_3, $NdCo_2$, $NdCo_3$, Nd_2Co_7, Nd_5Co_{19}, $NdCo_5$ and Nd_2Co_{17}.

The results of some preliminary sintering experiments using $NdCo_5$ and $DiCo_5$ as base metals and 60 Sm/40 Co and 70 Pr/30 Co alloys as sintering aids are reported. Intrinsic coercive forces of 4000 Oe and 8820 Oe

were obtained with the 70 Pr/30 Co sintering aid for $NdCo_5$ and $DiCo_5$, respectively. A peak coercive force of 10280 Oe was obtained for $DiCo_5$ sintered with 60 Sm/40 Co.

TABLE OF CONTENTS

TABLE OF CONTENTS
(continued)

LIST OF ILLUSTRATIONS

SECTION I

LIST OF ILLUSTRATIONS
(continued)

SECTION II

SECTION III

LIST OF ILLUSTRATIONS
(continued)

LIST OF ILLUSTRATIONS
(continued)

SECTION IV

SECTION I

MAGNETIC PROPERTIES OF $R_2(Co, Fe)_{17}$ PHASES

A. THERMOMAGNETIC ANALYSIS OF $R_2(Co, Fe)_{17}$ PHASES (Hartings, Mildrum, Strnat)

The thermomagnetic analysis of the quasi-binary systems R_2Co_{17}-R_2Fe_{17} has been substantially completed in the temperature range above 20°C by measuring the temperature dependence of the permeability in low ac fields. Preliminary results for the systems with R = Y, Sm and Ce were described in the last report, but some data was still missing at that time. The two systems with R = Y and Sm, now complete, are shown in Figure 1. No surprises were found.

In the iron-rich alloys of the yttrium system, the Curie point proper of the 2-17 phase is the only event seen in the TMA spectrum. It occurs at substantially the same temperature on heating and cooling and the Hopkinson maxima are of nearly equal height and shape. This is taken as an indication that these phases do not show the same tendency to decompose on prolonged heating at temperatures between 500-1000°C which appears to be present in the Fe-rich portions of the systems involving any of the other rare earth metals.

In the samarium system, TMA runs were repeated for several alloys on the iron-rich side, in the range from x = 0.6 to 1.0, and these runs were extended to higher peak temperatures. The unexpected high temperature events previously found in the middle of the composition range and between the temperatures of 900 and 1000°C continue to occur up to and including x = 1.0, the binary phase Sm_2Fe_{17}. The temperature of the event observed on heating drops gradually with increasing iron content to a value of 760°C at x = 1. The event is equally prominent on heating and cooling and shows no or only very little thermal hysteresis.

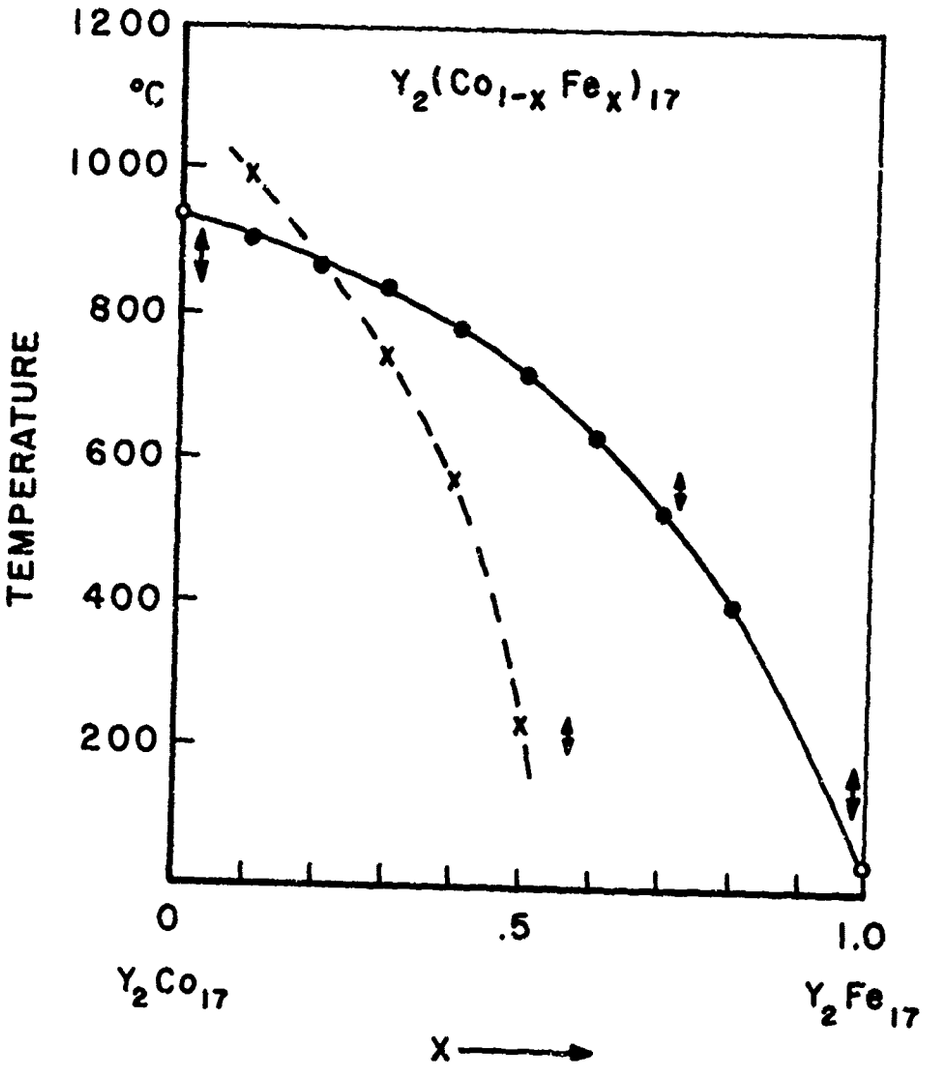

Figure 1a. Results of thermomagnetic analysis for the system Y_2Co_{17}-Y_2Fe_{17}.

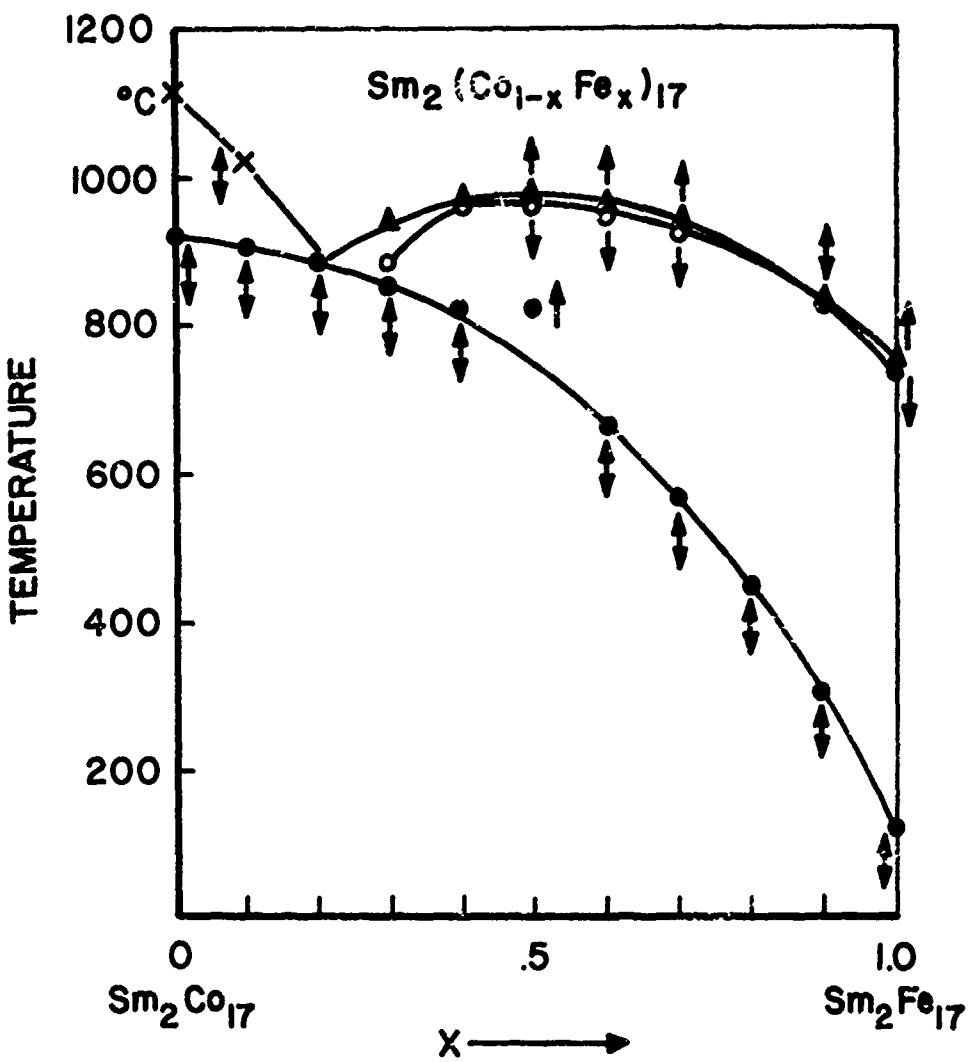

Figure 1b. Results of thermomagnetic analysis for the system Sm_2Co_{17}-Sm_2Fe_{17}.

The general outline of the cerium system has not changed from that shown in the previous report. However, a considerable amount of detailed analytical work has been done on this system, especially on the equiatomic alloy $Ce_2(Co_{0.5}Fe_{0.5})_{17}$, in an attempt to clarify the significance of the secondary magnetic transition points observed above the Curie temperature of the 2-17 phase. This particular system has been chosen for the detailed study because the secondary events occur here over the widest composition range and at relatively low temperatures (which makes experimentation more convenient), and since the thermal hysteresis of these events is by far most pronounced. The results to date of this analysis and the conclusions drawn from them are described in Section II of this report.

The TMA results for the systems in which the rare earth components are praseodymium and mischmetal, respectively, are shown in Figure 2. The secondary events at high temperatures are observed in both. As in the Ce system, this is probably attributable to the formation of a Co-Fe phase during the heating-cooling cycle and may indicate a tendency for alloys of the 2-17 phase in the iron-rich half of the systems to decompose by a eutectoid reaction. In the praseodymium system, this high temperature event is found only for $x \geqq 0.7$. At $x = 0.7$ it exhibits a thermal hysteresis of $\sim 20^{\circ}$. For $x \geqq 0.8$, the hysteresis disappears.

As may be expected, the situation in the mischmetal system is similar to that in the cerium system, but even more complex. For the Fe-rich alloys, a hysteretic high-temperature transition is observed which is analogous to that seen in the Ce system. But above it, still another TMA "event" is observed which does not exhibit a thermal hysteresis. It may be that mischmetal first forms a uniform 2-17 phase during the homogenization anneal, acting as if it were a single rare earth metal. During the initial, rapid cooling, this phase is quenched in and is responsible for the systematic composition dependence of the Curie point in the low temperature range (between 0 and $600^{\circ}C$). As this compound disassociates during the slow heating in the course of the TMA experiment, the main constituents of

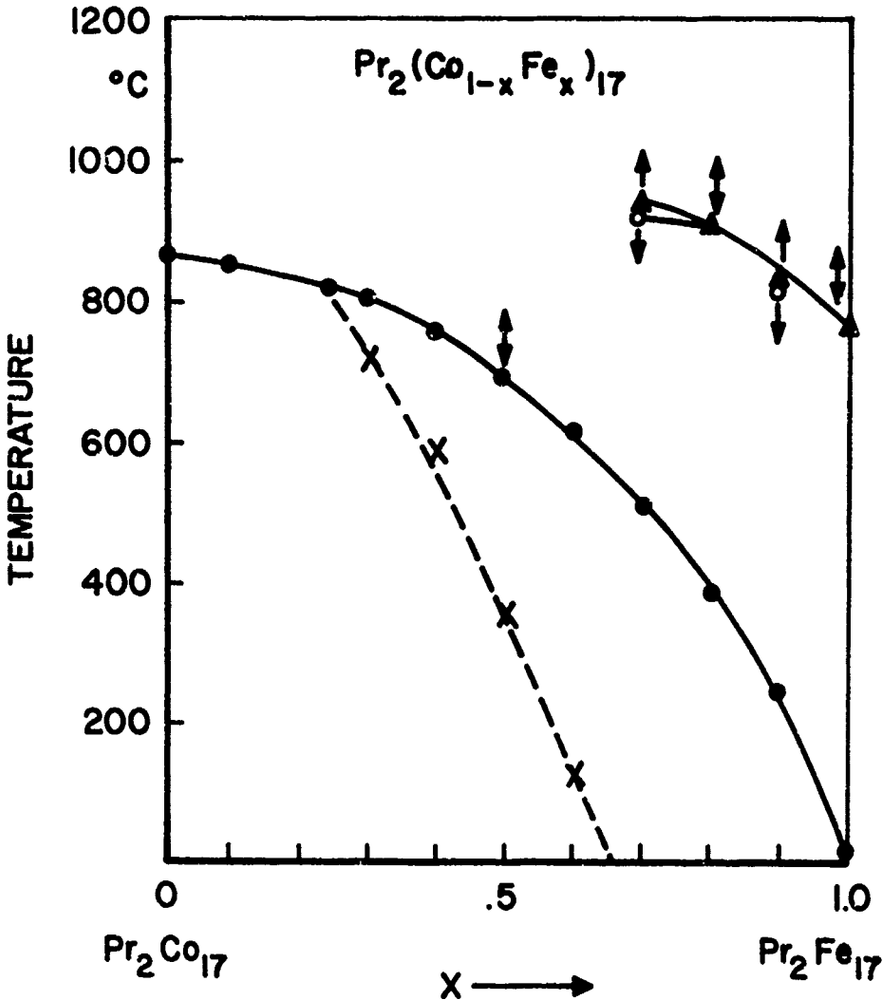

Figure 2a. Results of thermomagnetic analysis for the system Pr_2Co_{17}-Pr_2Fe_{17}.

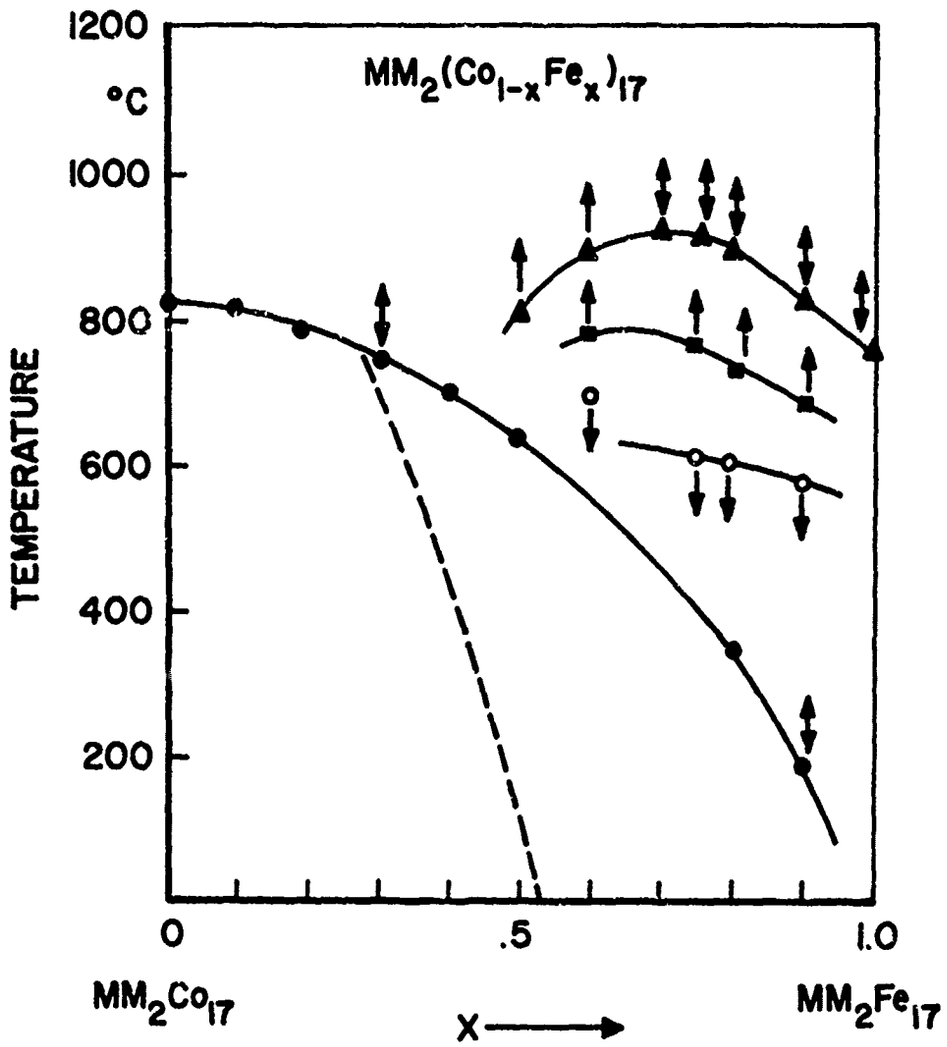

Figure 2b. Results of thermomagnetic analysis for the system MM_2Co_{17}-MM_2Fe_{17}.

the mischmetal, cerium and lanthanum, may partition because of the different stability of their respective 2-17 compounds, leading to a disappearance of the magnetic order in two discrete stages, at temperatures which differ between 100 and 200°C. However, mischmetal is a multicomponent alloy, and the $MM_2(Co_{1-x}Fe_x)_{17}$ system is consequently a very complex one. An understanding of the thermal and thermomagnetic events observed on these alloys must wait until after the results found in the simpler cerium system have been explained.

It is noteworthy that in both the Pr and MM system shown here, another event is observed on the Co-rich side which drops rapidly with increasing Fe content to levels near room temperature for the compositions x = 0.6 and 0.5, respectively. This is quite analogous to the minor event observed for all alloys in the cobalt-rich half of the yttrium system. There, we tentatively ascribed this "wiggle" to the presence of a minor amount of an impurity phase which is an Fe-Co alloy stabilized in its austenitic form by the presence of a small amount of rare earth. This minor thermomagnetic event is only observed in cobalt-rich alloys, while the very prominent and strongly hysteretic high-temperature events are found only on the iron-rich side. The two appear to be mutually exclusive. Our working hypothesis assumes that both events are attributable to an Fe-Co phase which, for the cobalt-rich alloys, appears to be present from the beginning in an amount which does not change in the course of the experiment, while for the iron-rich alloys it is formed during the experiment at the expense of the 2-17 phase, presumably by the eutectoid decomposition of the latter. However, the fact that this "wiggle" becomes very prominent in several Pr and MM alloys causes conceptual problems.

Future work with the thermomagnetic analysis apparatus will concentrate on attempts to clarify the meaning of this multitude of magnetic transitions. This will require the study of judiciously selected alloys with several analytical tools in a mutually complimentary way. These experiments will be conducted with Ce-Co-Fe and Y-Co-Fe alloys. Thermomagnetic

analysis will also be extended to temperatures below room temperature. This is of primary interest for the iron-rich alloys, particularly those in the yttrium and cerium systems.

B. MAGNETIC SATURATION MEASUREMENTS ON $R_2(Co, Fe)_{17}$ (Mildrum, Tront, Strnat)

Room temperature magnetization measurements were made with the oscillating specimen magnetometer. The samples were powders prepared by mortar grinding with a particle size < 37 μm. A small quantity of the powder, typically 40 mg, was precisely weighed and encapsulated in a sample holder which confined the particles to a small cylindrical volume of approximately 3 mm diameter x 3 mm long. The powder was loosely packed in such a way the particles were free to rotate in an applied magnetic field and thus to align their easy axis of magnetization with that field, while being confined to a small and well-defined volume in which they could not shake around freely. Magnetization-vs.-applied field curves were measured in fields up to 20 kOe. Figure 3 shows two magnetization curves measured in this manner which constitute the best and the worst case incurred with respect to the degree of saturation achieved. The experimental objective of this measurement was to obtain a sufficiently long horizontal portion of the high-field magnetization curve that one could be sure that technical saturation had been achieved. This was found to be reasonably well the case for all samples measured. Saturation magnetization values were then calculated from the magnetometer readings at the highest field. The initial, low-field part of the magnetization curve measured is meaningless, since it is not possible in this range to separate magnetization changes occurring within the particle from those which are due to physical rotation of the grains.

The results of these room-temperature magnetization measurements for the system in which the rare earth is yttrium, cerium, praseodymium, neodymium and samarium are summarized in Figures 4 through 8. Measurements for the mischmetal system are still quite incomplete due to

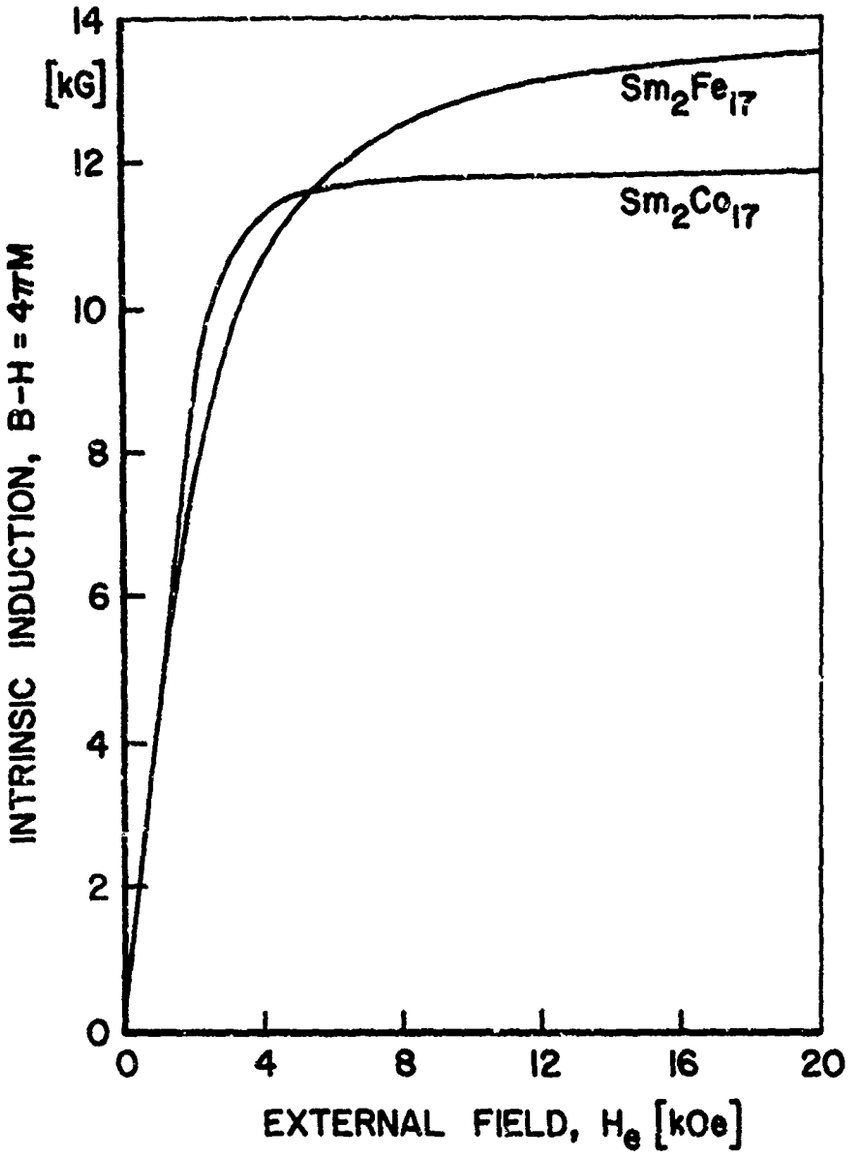

Figure 3. Magnetization curves measured on loose-powder samples of Sm_2Co_{17} and Sm_2Fe_{17}.

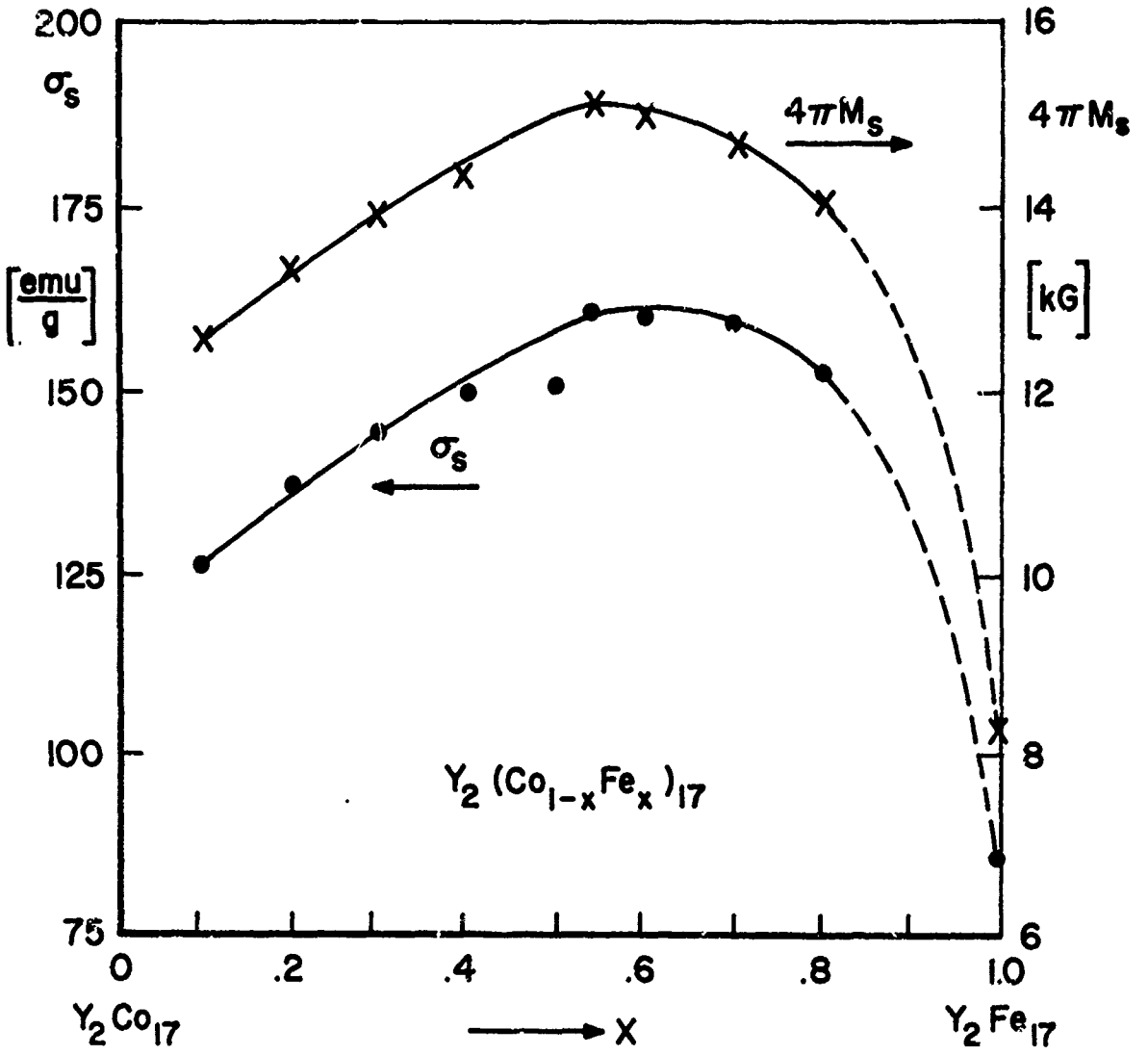

Figure 4. Room-temperature "technical saturation" of $Y_2(Co_{1-x}Fe_x)_{17}$ alloys.

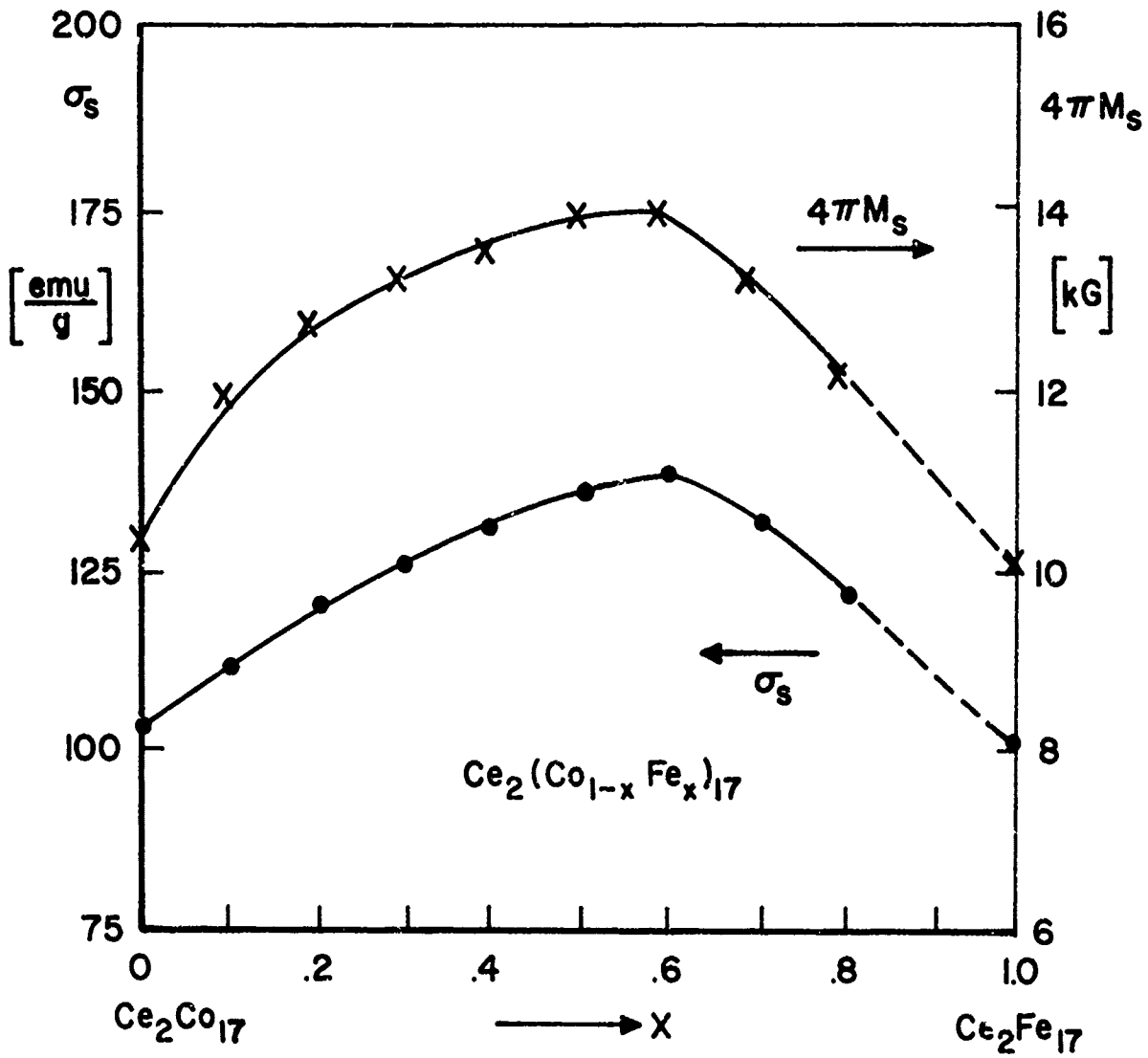

Figure 5. Room-temperatur "technical saturation" of $Ce_2(Co_{1-x}Fe_x)_{17}$ alloys.

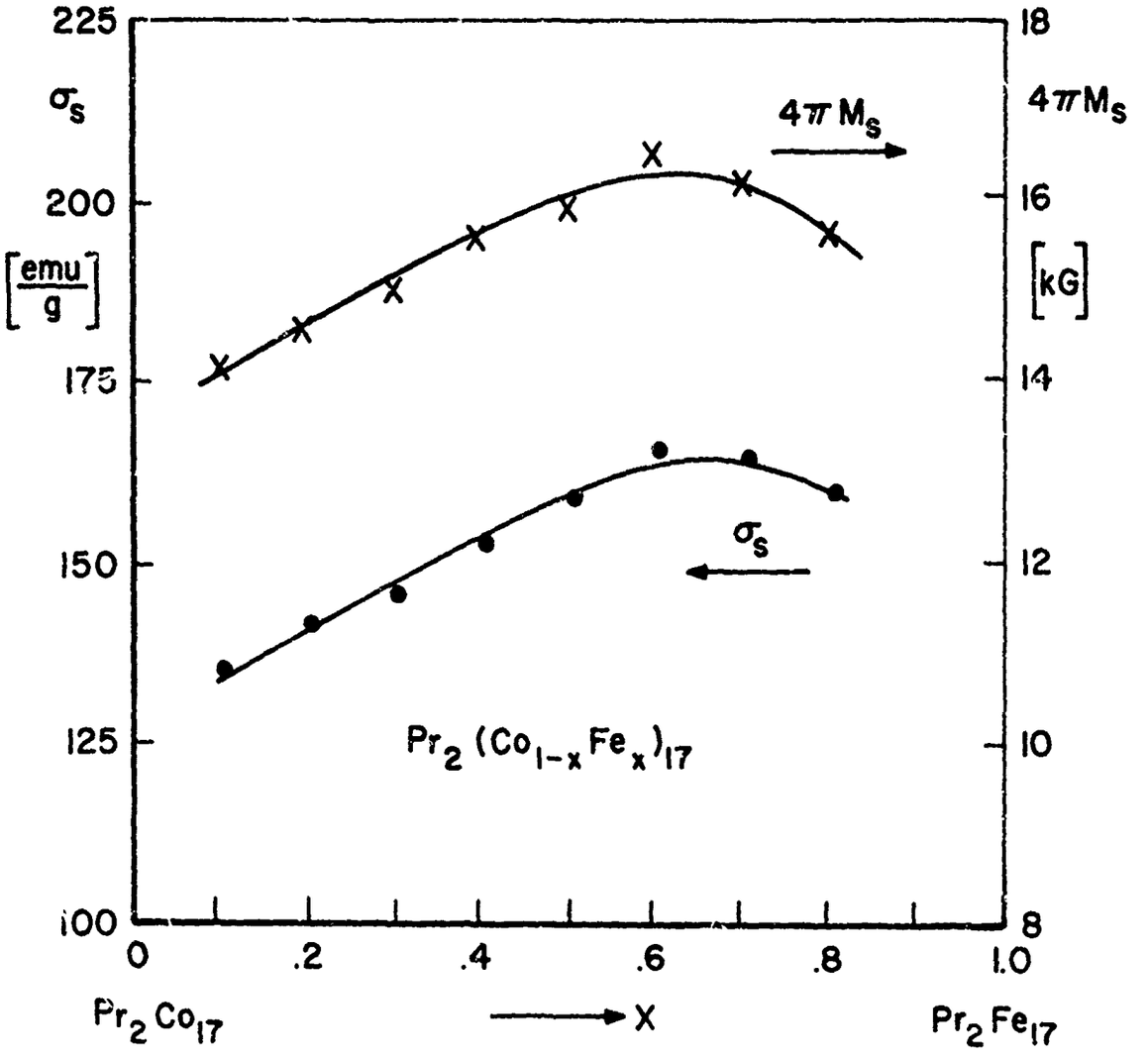

Figure 6. Room-temperature "technical saturation" of $Pr_2(Co_{1-x}Fe_x)_{17}$ alloys.

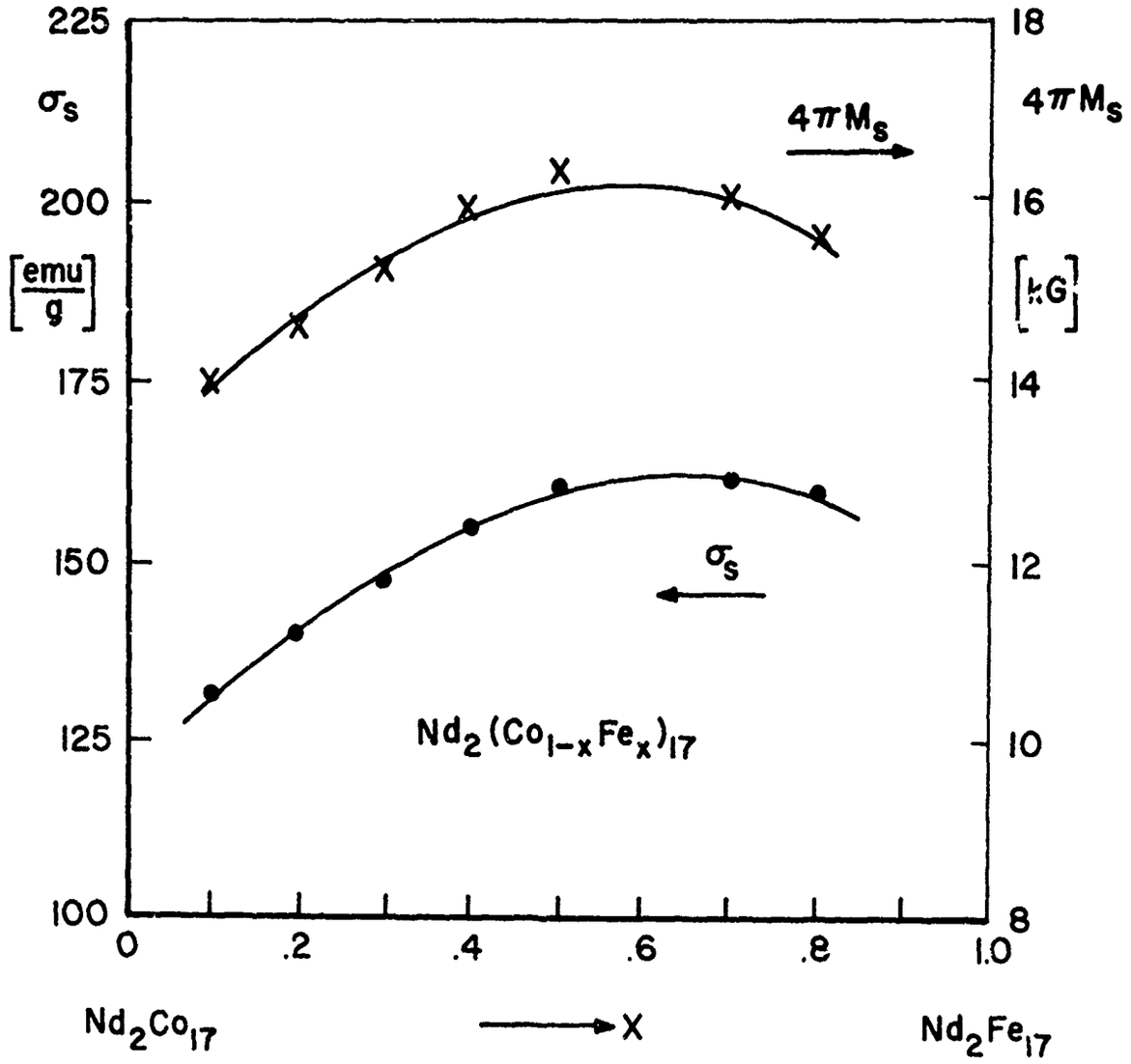

Figure 7. Room-temperature "technical saturation" of $Nd_2(Co_{1-x}Fe_x)_{17}$ alloys.

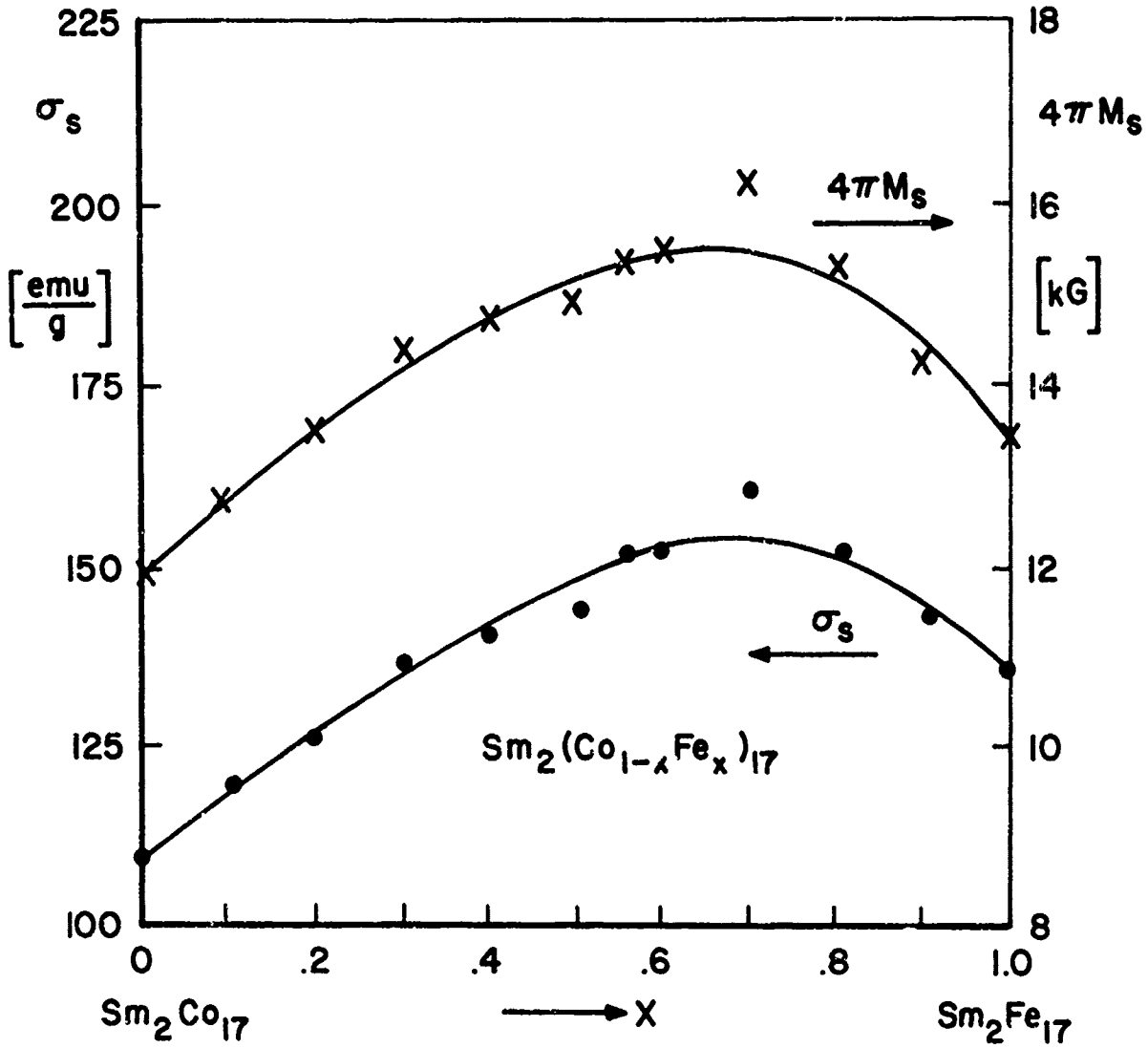

Figure 8. Room-temperature "technical saturation" of $Sm_2(Co_{1-x}Fe_x)_{17}$ alloys.

the fact that a number of the alloys which had been measured initially turned out to contain considerable quantities of other phases. We are in the process of repeating these measurements and will report the results at a later date. The data are presented in two ways: as intrinsic induction $4\pi M_s$, in units of Gauss (magnetic moment per unit volume) and as specific magnetization in the CGS system, expressed in emu/g (magnetic moment per unit weight).

Inspection of the graphs shows that in all these systems, the room temperature saturation rises with increasing iron content throughout the composition regions in which easy c-axis anisotropy was observed and which are of interest for the potential permanent magnet application. In each system, a maximum occurs for values of x between 0.5 and 0.7 which is followed by a decrease of σ with further increase of x. This maximum shifts slowly toward higher iron contents with increasing atomic number of the rare earth metal. This is a consequence of the rapid increase of the Curie temperature of the R_2Fe_{17} compounds with increasing atomic number of R and was to be expected. The maximum value of the saturation found in the samarium system is approximately 16,300 Gauss for $Sm_2(Co_{0.3}Fe_{0.7})_{17}$, in the praseodymium system it is 16,550 Gauss for the alloy $Pr_2(Co_{0.4}Fe_{0.6})_{17}$.

C. CRYSTAL ANISOTROPY OF $Sm_2(Co, Fe)_{17}$ PHASES

For the purpose of estimating the magnitude of the magnetocrystalline anisotropy of the rare earth-cobalt-iron phases of 2-17 stoichiometry, magnetically aligned powder samples were prepared of all the single phase alloys available. In the composition range in which the crystallographic c-axis is the easy direction of magnetization, such samples can be used to simulate single crystals, and it is possible to estimate the values of the first and second order anisotropy constants from magnetization measurements made on these powder samples. To do this, we measure on each sample a pair of magnetization curves, with the field applied once in the direction of the particle alignment and once perpendicular to it. These will

be referred to as the easy-axis and hard-axis magnetization curves in the following paragraphs.

Such measurements have been performed on a large number of alloys from the systems with R = Sm, Pr, Ce, Y, and MM. In each case, the entire range of compositions in which easy c-axis behavior was previously found by an x-ray diffraction technique was covered. These measurements have fully confirmed the conclusions drawn on the basis of the few selected curves measured before and shown in the last progress report, namely, that by far the highest anisotropy is found in the samarium system, a situation quite analogous to that which exists in the RCo_5 compound family. In this chapter, we show additional magentization curves measured on cobalt-rich Sm-Co-Fe alloys, and we attempt to analyze the data for the entire easy-axis range of the samarium system in terms of anisotropy constants and anisotropy fields.

Figure 9 shows the pairs of magnetization curves measured on powder samples of Sm_2Co_{17} and $Sm_2(Co_{0.9}Fe_{0.1})_{17}$. The measurements were done at room temperature using the oscillating specimen magnetometer. The source of the magnetizing field was a 9-inch Varian electromagnet which provides a maximum field of 20 kOe at the required gap width. This field was by far insufficient to produce saturation in the hard direction of magnetization. Only about 40% of the saturation magnetization could be achieved. Qualitative inspection of the curves shows that the substitution of 10% of the cobalt by iron does not significantly affect the anisotropy. If anything, the hard-axis curve becomes slightly flatter, and since the saturation magnetization is raised by about 5%, the anisotropy field defined as the field needed to saturate the sample in the hard direction should rise by about the same percentage. Figure 10 shows an equivalent set of curves measured on samples of $Sm_2(Co_{0.8}Fe_{0.2})_{17}$ and $Sm_2(Co_{0.7}Fe_{0.3})_{17}$. The saturation continues to increase with increasing iron content, but now the initial slope of the hard-axis curve also increases, indicating a drop of the first-order anisotropy constant, K_1.

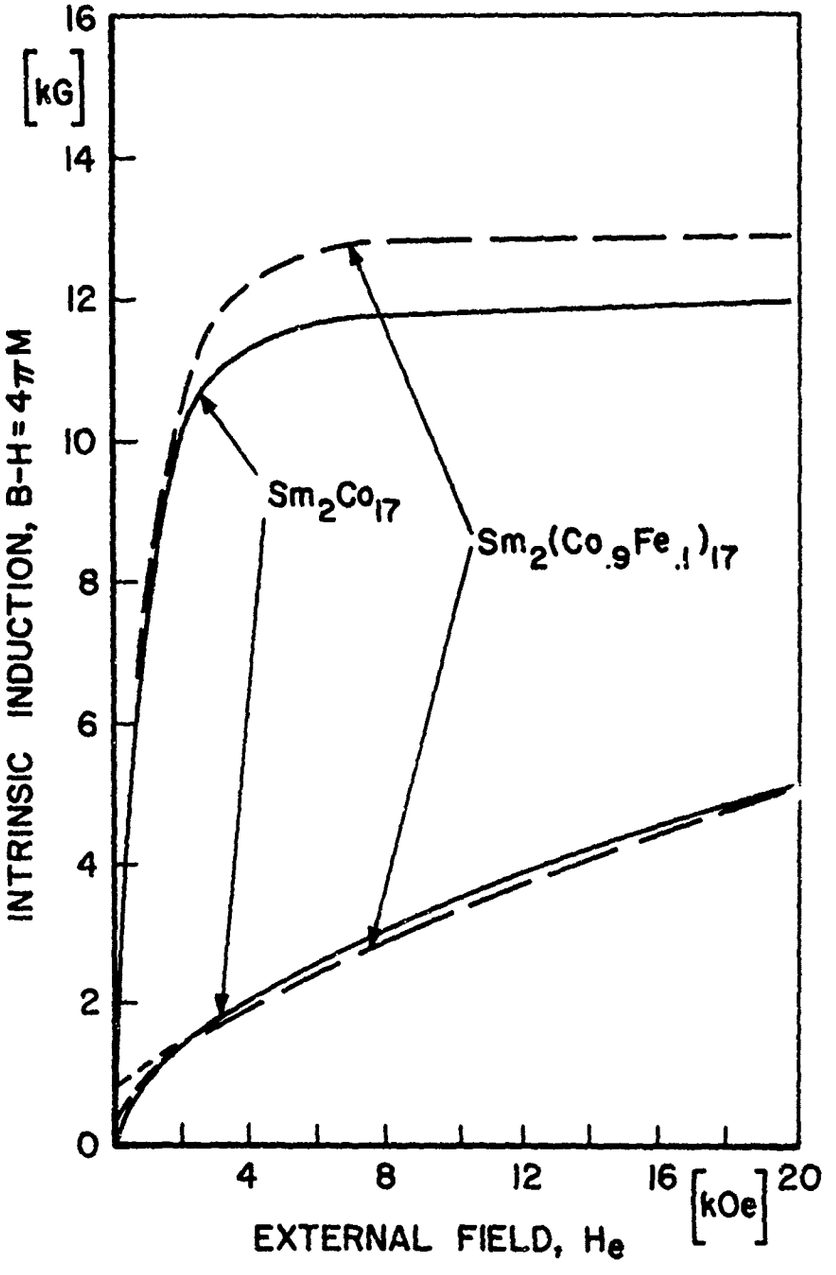

Figure 9. Easy and hard-axis magnetization curves measured on aligned powders of $Sm_2(Co_{1-x}Fe_x)_{17}$ phases with x = 0, 0.1.

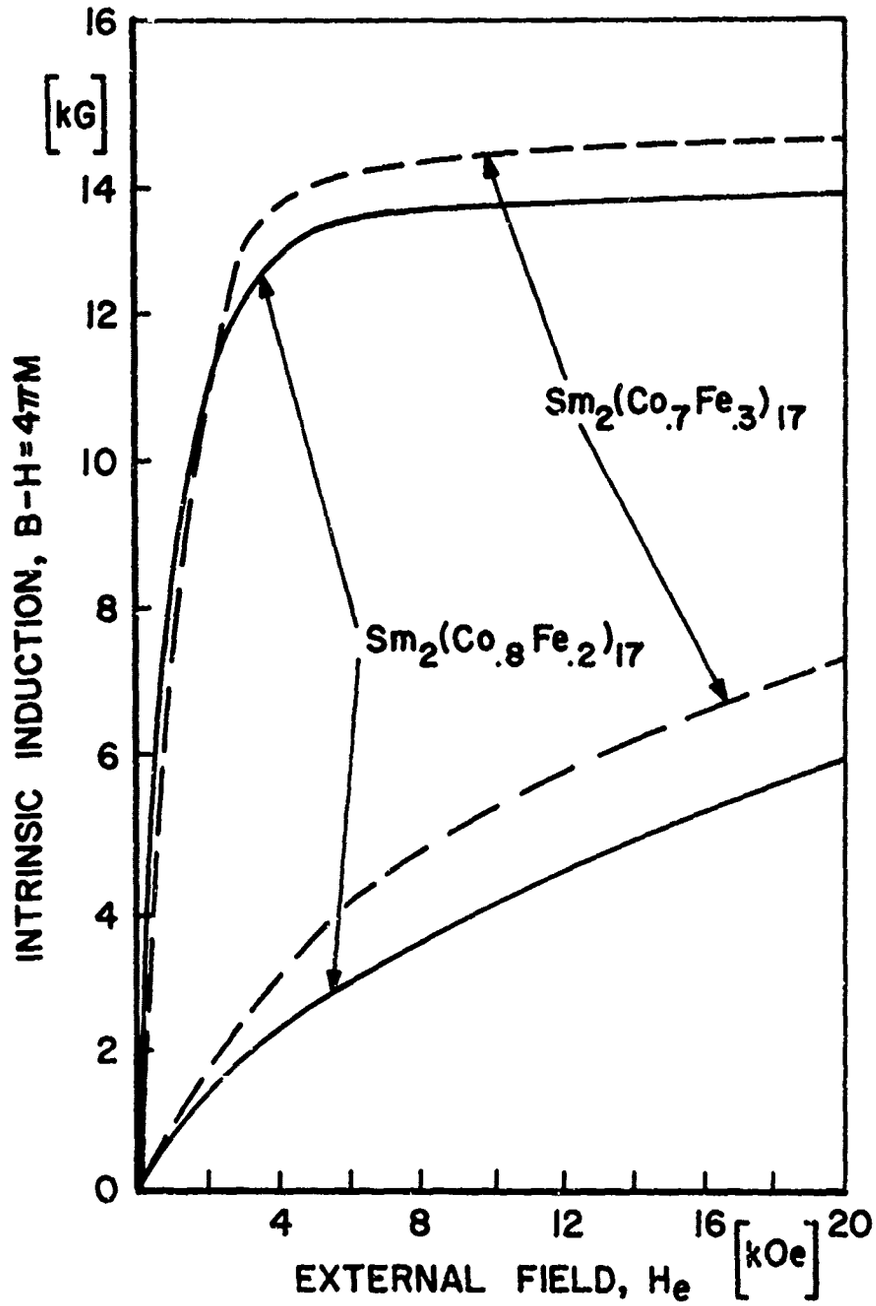

Figure 10. Easy and hard-axis magnetization curves measured on aligned powders of $Sm_2(Co_{1-x}Fe_x)_{17}$ phases with x = 0.2 and 0.3.

The anisotropy constants are derived from an analysis of the shape of the hard-axis curve which was first applied to single crystal measurements on cobalt by Sucksmith and Thompson[1]. The formulae derived by them are applicable to curves measured on aligned-powder samples if one can indeed be sure that the crystallographic c-axis is the easy direction of magnetization. Only the uniaxial anisotropy constants, K_1 and K_2, which describe the differences in the energy of magnetization between the c-axis and the basal plane, can be derived from aligned-powder sample measurements. It is not possible to obtain any information about a basal-plane anisotropy which may also be present. For this, single crystals will be required. It must furthermore be noted that the uniaxial anisotropy constants obtained in such a manner are only approximations and that a precise determination of these will also have to await single-crystal measurements. The reasons are that even particles of < 37 μm diameter, as we use them in our measurements, may consist of more than one grain and thus may not be single crystals. Furthermore, the irregular external shape of the particles and the friction forces between them prevent perfect alignment in an orienting field.

These problems are illustrated with Figure 11 which shows a pair of magnetization curves measured by us on aligned powder of $SmCo_5$ and, for comparison, single-crystal data for the same compound published by Buschow and Velge[2]. It is seen that the alignment problems mentioned primarily affect the initial low-field portion (to about 2 kOe) of the hard-axis magnetization curve, which is strongly concave for the powder measurement but straight for the measurement taken on the single crystal. However, the analysis of such powder measurements nevertheless allows a reasonably good estimate of the first anisotropy constant, K_1, and an even better approximation of K_2 provided a reasonably long portion of the hard-axis curve is available, as it is for the 2-17 phases. In the case of K_1 or the combined uniaxial anisotropy constant, $K_1 + K_2$, the method should provide a lower limit. The actual values of these quantities should be slightly higher

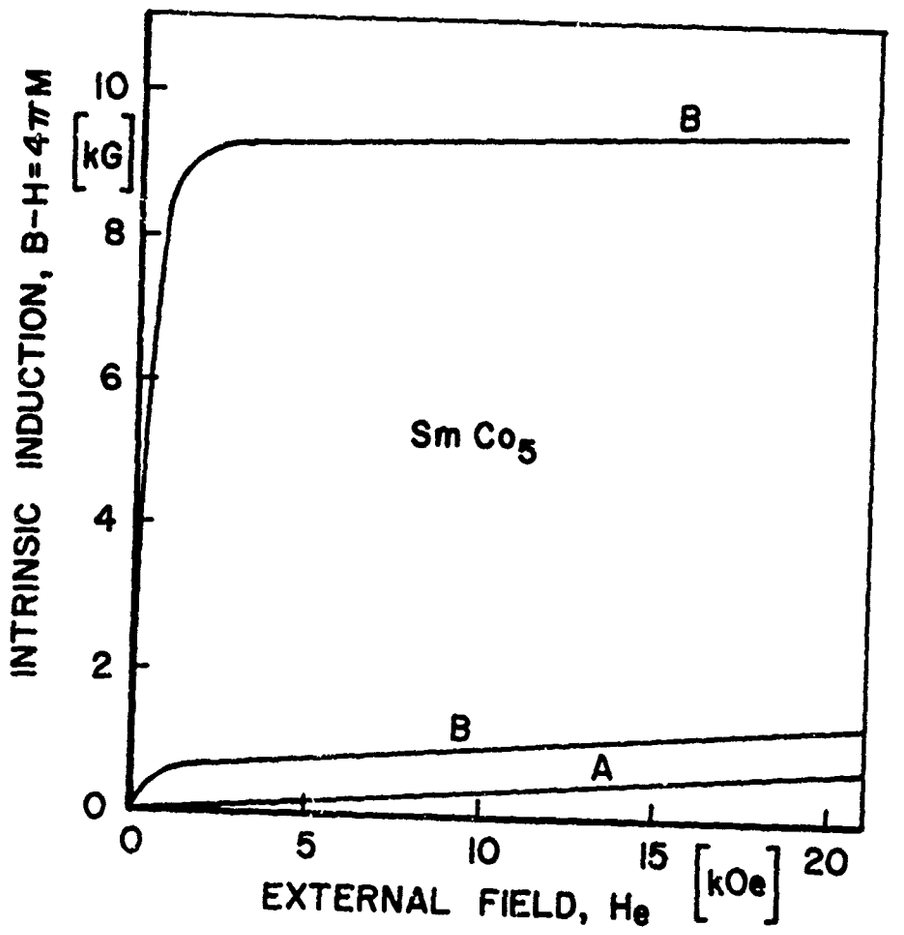

Figure 11. Comparison of easy and hard-axis curves measured on a single crystal (Curve A) and aligned powder (Curve B) of $SmCo_5$.

than the ones we determined here. Note that the value of $K_1 + K_2$ determines an anisotropy field, $H_A = 2(K_1 + K_2)/M_s$, which is considered to be a theoretical upper limit of the coercive force of small particles[3].

The magnetization curves are plotted in terms of the externally applied field; no attempt has been made to correct for demagnetizing fields. It is very difficult to know which value of the demagnetizing factor should be used if such a correction were attempted. During alignment in a field, the magnetic particles in the epoxy matrix arrange basically in long chains, running from pole to pole in the direction of the orienting field. These chains repel each other in the direction perpendicular to that field and, consequently, distribute themselves in a reasonably evenly-spaced pattern across the sample cross section. The demagnetizing factor, N, for the easy-axis curve should thus be quite low, while N is definitely higher when the field is applied perpendicular to the long direction of the chains. However, it seems that the demagnetizing factor for a cylinder magnetized perpendicular to its axis ($N = 2\pi$ in the CGS system) is too high in view of the fact that the sample consists of many such cylinders in close proximity to each other. It may be said, however, that for the relatively high-anisotropy substances, which all of these Sm-Co-Fe compounds are, the demagnetizing field is a rather small fraction of the applied field, and the error incurred by not making a demagnetization correction is a minor one. However, contrary to the error incurred due to the use of powder samples instead of single crystals, the neglect of a correction for self-demagnetization leads one to overestimate the anisotropy field. In the later analysis of other, lower-anisotropy substances, it will not be permissible to simply disregard the demagnetizing field.

Figure 12 illustrates the procedure used in determining the anisotropy constants K_1 and K_2 from the hard-axis magnetization curve, using as an example Sm_2Co_{17}. The measured M vs. H-data is replotted as H/M vs. M^2. When this is done the lower set of points, represented by solid dots, results. For the higher values of M^2, these points lie on a straight line which is

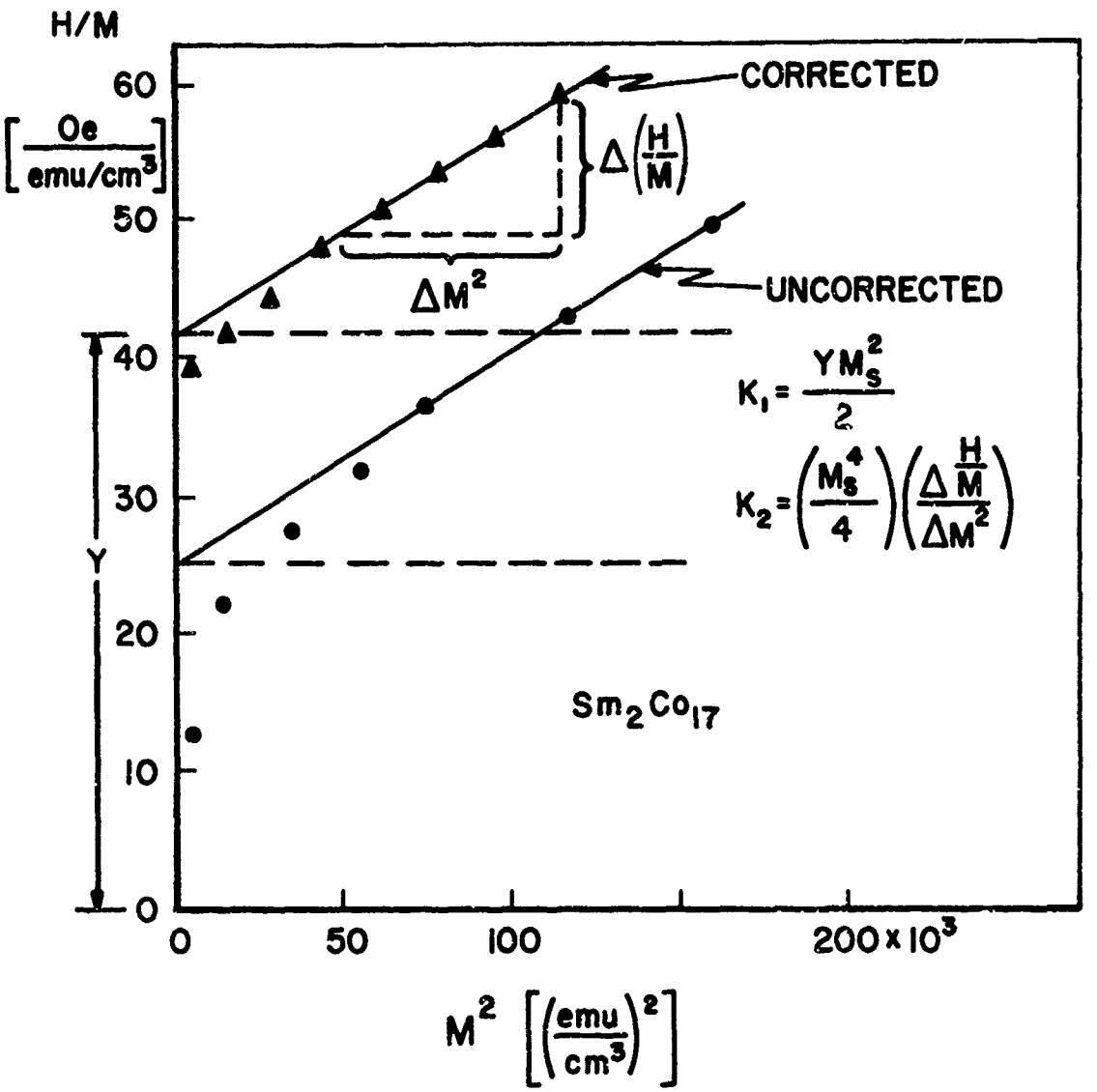

Figure 12. Determination of anisotropy constants for Sm_2Co_{17} from the hard-axis magnetization curves.

shown in the graph and marked "uncorrected". The intercept of this straight line, Y, with the ordinate axis allows one to determine K_1 from the relation $K_1 = YM_s^2/2$. The slope of the line is related to the second-order anisotropy constant, $K_2 = (M_s^4/4) \cdot [\, \Delta(H/M) / \Delta M^2 \,]$. In view of the difference seen in Figure 10 between the hard-axis curves of a powder and a single-crystal sample, we can expect that a similar additional curvature of the hard-axis curve in the low-field range up to 2 or 3 kOe is present also in the powder curves for Sm_2Co_{17} and all of the others analyzed here. We felt justified in applying a correction for this fact. This is done by extrapolating the higher-field portion of the hard-axis curve (H >2 kOe to H = 0), as is indicated by the dotted line in Figure 9. If the intercept of this extrapolated curve with the y-axis is taken as the new origin and the H and M data of this fictitious hard-axis magnetization curve are transformed accordingly, the higher-lying set of points (triangles) and the straight line marked "corrected" in Figure 12 result. This correction affects primarily the intercept with the H/M axis and consequently K_1. The slope of the curve, and therefore K_2 are essentially unchanged by this correction. The anisotropy constants and anisotropy-field values listed later are determined by applying this mathematical analysis and correction procedure in an analogous way to all the hard-axis curves measured. While the extrapolation of the low-field portion of the curves is somewhat arbitrary, we feel that a better estimate of the first-order anisotropy constant results by using this procedure.

Figure 13 shows replots of the hard-axis magnetization curves for the iron-substituted compounds $Sm_2(Co_{1-x}Fe_x)_{17}$ for the values x = 0.1, 0.2, 0.3 (from Figures 9 and 10) x = 0.4 and 0.5 (see Figure 9, p. 20 of AFML-TR-72-99). The values of K_1 and K_2 determined in this manner are summarized in the Figure 14. Also shown in this graph as a function of composition are the total uniaxial anisotropy constant, $K_1 + K_2$, and the anisotropy field calculated from it, $H_A = 2(K_1 + K_2) / M_s$. Also shown are values for an anisotropy field, H_A', which is determined by linear

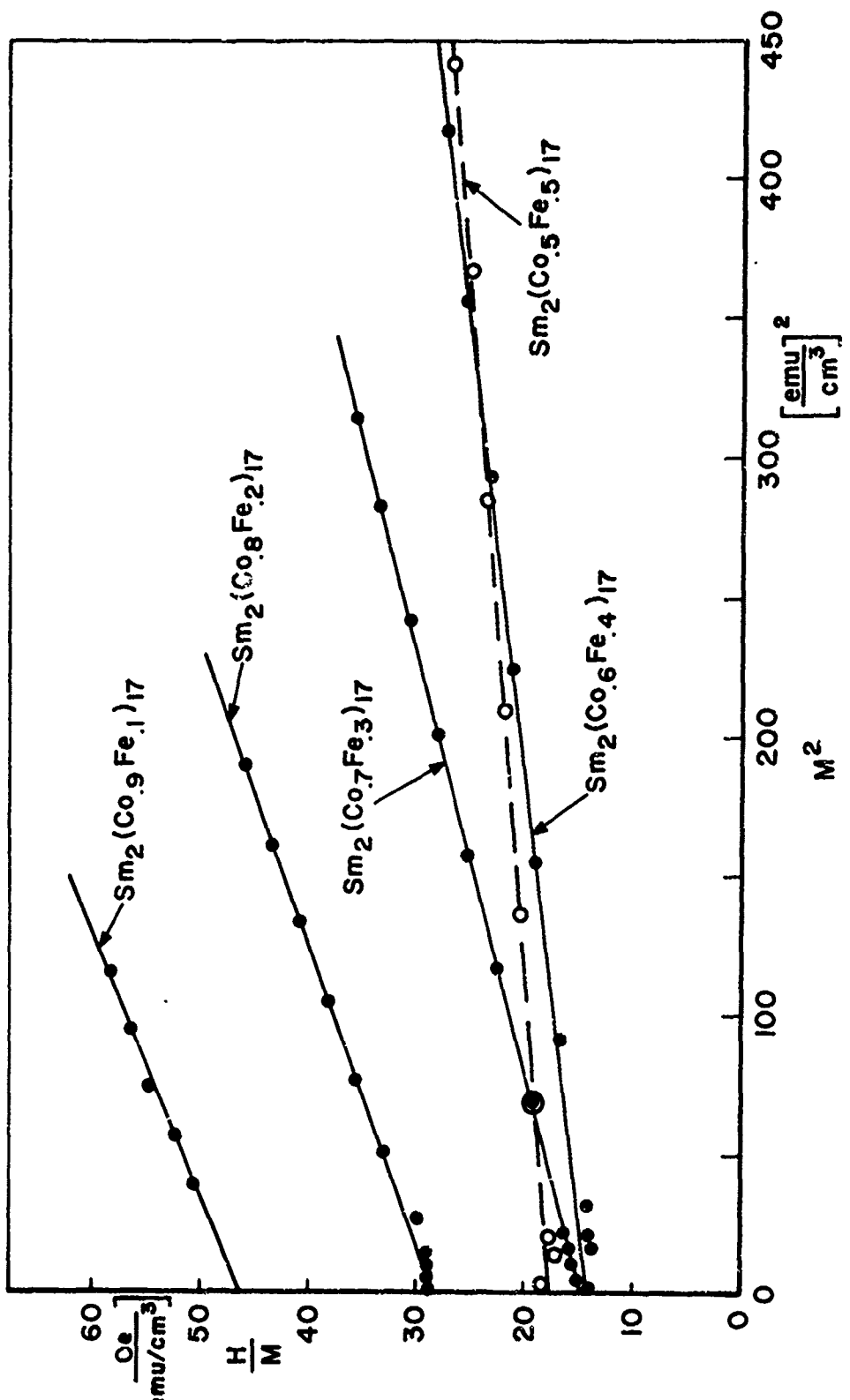

Figure 13. Determination of anisotropy constants for $Sm_2(Co_{1-x}Fe_x)_{17}$ with x = 0.1-0.5 from the hard-axis magnetization curves.

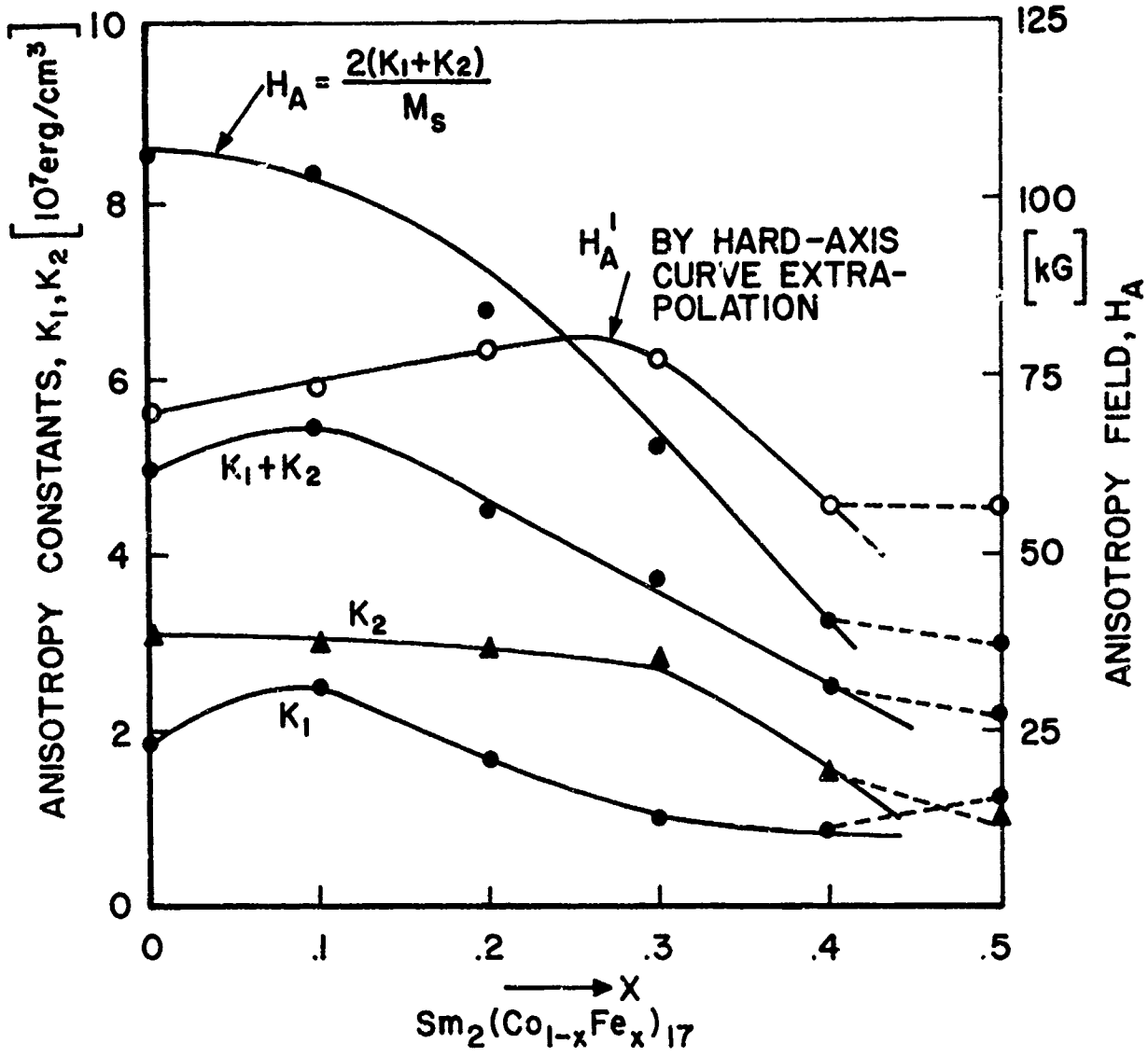

Figure 14. Anisotropy constants and anisotropy field values in the system $Sm_2(Co_{1-x}Fe_x)_{17}$.

extrapolation of the hard-axis magnetization from H = 20 kOe to the intercept with the saturated portion of the easy-axis curve. The point illustrated for the x = 0.5 composition does not follow the normal trend of the curves. We have suspected (from our TMA data) that this alloy was unaccountably prepared having an x = 0.4 composition. A new alloy of x = 0.5 will be prepared and experimental results presented in succeeding reports. It can be seen that the addition of iron at first only slightly affects the anisotropy field and may even raise it a little, while larger iron substitutions tend to lower it.

Throughout the entire composition range in which these measurements were made, the anisotropy remains high enough that it should be possible to obtain practically useful coercive forces of several thousand Oersteds with properly prepared fine powders of these substances. If the previous experience with RCo_5 compounds, barium ferrite, MnBi and other crystal-anisotropy magnet materials can serve as a guide, one may expect to realize intrinsic coercive forces of 10 to 15% of the anisotropy-field values, i.e., in the range from 5 to 15 kOe.

REFERENCES

1. W. Sucksmith and J. E. Thompson, Proc. Royal Soc. (London), v. 225 (1954) p. 362.

2. K. H. J. Buschow and W. A. J. J. Velge, Z. angew. Physik, v. 26 (1969) p. 157.

3. E. P. Wohlfarth, Advances in Physics, v. 8 (1959) p. 87.

SECTION II

STUDY OF THE LOW TEMPERATURE INSTABILITY OF $Ce_2(Co_{0.5}Fe_{0.5})_{17}$*

A. INTRODUCTION

In the previous report[1] and in Section I of this report, we have reported the unusual TMA spectra of the $Ce_2(Co_{1-x}Fe_x)_{17}$ alloys, especially those with $0.4 \leq x \leq 0.7$. A summary of magnetic transitions observed for the $Ce_2(Co, Fe)_{17}$ phases is repeated in Figure 1a. In Figure 1b are repeated the thermal events observed by DTA for the same series of alloys[2]. It has been noted that the TMA and DTA results for the Curie temperatures of the $Ce_2(Co, Fe)_{17}$ phases are in very close agreement. It has also been noted that both sets of measurements are in close agreement on the temperatures at which another event(s) occurs between 800°C and 900°C for $0.4 \leq x \leq 0.7$. For the DTA measurements, which preceded the TMA results, it was proposed that these high temperature thermal events were due to a disordering of the Co and Fe positions in the $Ce_2(Co, Fe)_{17}$ lattice. In retrospect, this interpretation should have been suspect since the observed thermal events were much too intense and well-defined to be explained by a typically second order transition. It was suggested that the complex magnetic behavior observed by TMA could be due to an instability of the $Ce_2(Co, Fe)_{17}$ alloys between 750°C and 850°C, but the relationships between the proposed decomposition products, a $Ce(Co, Fe)_2$ phase and a Co-Fe solid solution alloy, and the magnetic and thermal events were not obvious.

The major problem was to explain how any of the possible phases present could undergo a magnetic transition which was also accompanied by a sharply defined thermal event involving a large latent heat at temperatures

---

* Ray, Harmer, Geis

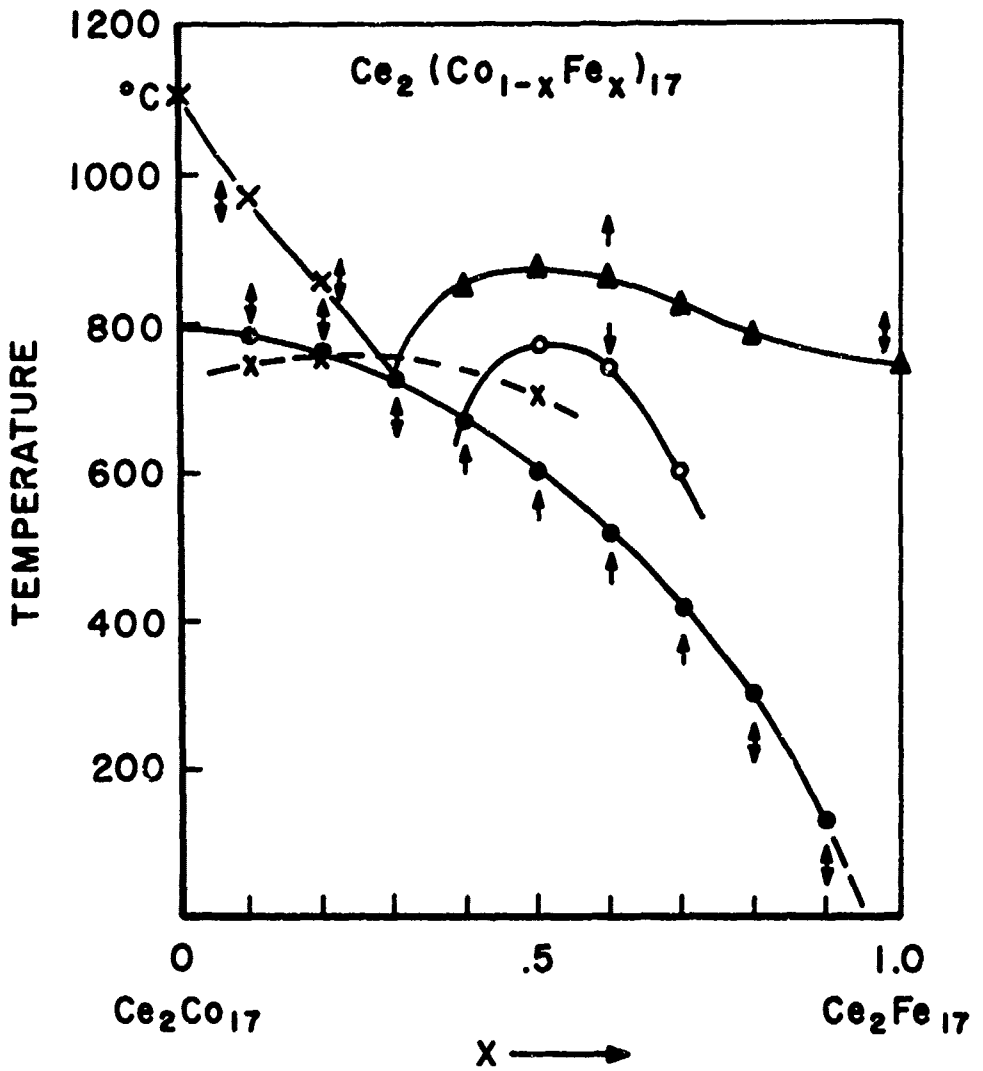

Figure 1a. Summary of magnetic transitions observed by TMA for $Ce_2(Co_{1-x}Fe_x)_{17}$ alloys.

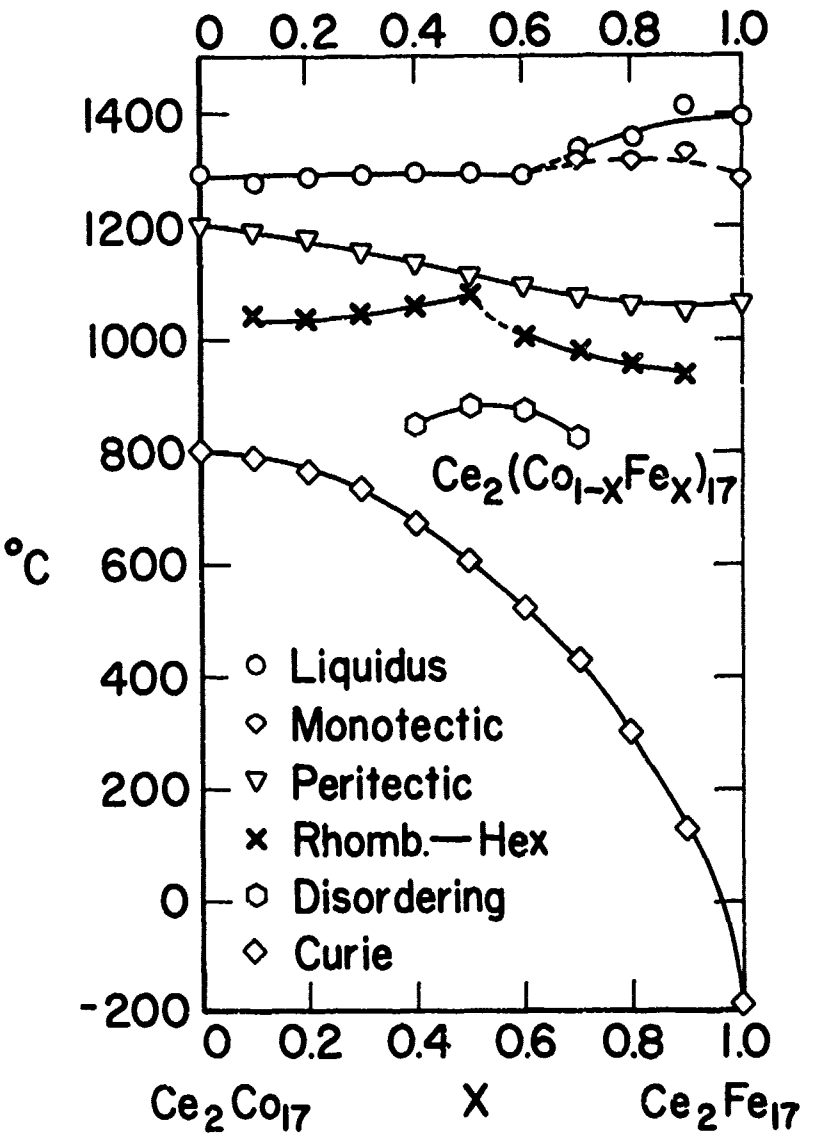

Figure 1b. Summary of the thermal events observed by DTA for $Ce_2(Co_{1-x}Fe_x)_{17}$ alloys.

between 820°C and 880°C. Finding a new phase in a ternary system unrelated to any of the binary systems is a highly improbable event, and the only other phase that could possibly be present that has a magnetic ordering temperature above 800°C would be a Co-Fe alloy. But, in the composition range where the magnetic transition and the bcc to fcc transformation of the Co-Fe alloys coincide, the transformations occur above 900°C.

We have carefully re-examined the DTA and TMA traces of three different alloys with the same nominal composition, $Ce_2(Co_{0.5}Fe_{0.5})_{17}$, and have prepared additional alloys with the same composition for additional metallography, electron microprobe analysis, and x-ray diffraction analysis. Although some experiments are still in progress, we believe we have found at least a reasonable explanation for the unusual behavior of these alloys.

B. RESULTS

Metallography and x-ray diffraction results obtained from three alloys with the same nominal composition, $Ce_2(Co_{0.5}Fe_{0.5})_{17}$, were reviewed. The results are given in Table I. From these results, it is obvious that the ternary phase, $Ce_2(Co_{0.5}Fe_{0.5})_{17}$ is stable at 1050-1100°C and that it can be retained at room temperature by fairly rapid cooling. We have determined that the hearth plate in the vacuum furnace used to anneal these alloys cools at an average rate of 50°C per minute between 1100°C and 500°C when the power to the heating elements is shut off abruptly.

A review of the DTA and TMA traces on these alloys revealed the following.

(1) The first event observed by either DTA or TMA occurs between 583°C and 601 C. Cycling from just above this event to 500°C then back weakens this event.

(2) The next event observed by DTA occurs between 661°C and 673°C. This is apparently a second order transition since it is not sharp but similar

TABLE I

SUMMARY OF METALLOGRAPHIC AND X-RAY DIFFRACTION RESULTS FOR THREE $Ce_2(Co_{0.5}Fe_{0.5})_{17}$ ALLOYS

Alloy No.	Heat Treatment	Lattice Constants*	Metallography
AR-785	7 hrs at 1050°C	a = 8.446 Å c = 12.433 Å	single phase
AR-837	18 hrs at 1100°C	a = 8.450 Å c = 12.431 Å	single phase
AR-853	65 hrs at 1050°C	a = 8.449 Å c = 12.434 Å	single phase

* Rhombohedral Th_2Zn_{17}-type structure, only phase observed.

in appearance to a Curie transformation. Cycling to 500°C from below 850°C and reheating strengthens this thermal event while heating above the reaction in the range of 851°C - 879°C weakens it. No magnetic transition corresponding to this DTA event is observed by TMA.

(3) A very intense event is observed between 851°C and 879°C by both DTA and TMA on heating, but in neither case is the reverse reaction observed.

(4) On cooling from above the event in the range of 851°C - 879°C, the first event observed by TMA occurs between 672°C and 765°C. The temperature at which this event is observed appears to depend on the maximum temperature to which the alloy is heated, with higher heating temperatures yielding lower transition temperatures. This is an intense TMA event. There is a corresponding DTA event but it is much weaker.

(5) If the maximum temperature to which the alloy is heated reaches 980°C or higher, the magnetic and thermal event in the range of 583°C - 601°C reappears.

A new alloy with the nominal composition $Ce_2(Co_{0.5}Fe_{0.5})_{17}$ was prepared by arc melting, homogenized at 850°C for 48 hours, then cooled to room temperature. Metallography of this alloy showed two phases present in nearly equal amounts. X-ray diffraction analysis showed one phase to be a bcc Co-Fe alloy with a = 2.862 Å, the other a $Ce_2(Co, Fe)_7$ phase with a = 4.996 Å, and c = 24.85 Å. Electron microprobe analysis of this alloy confirmed the x-ray analysis and showed the Co-Fe alloy to contain 37 at.% Co-67 at.% Fe, and the second phase to contain 22.11 at.% Ce, 57.8 at.% Co, and 20.1 at.% Fe. (A stoichiometric $Ce_2(Co, Fe)_7$ phase would contain 22.2 at.% Ce.)

C. INTERPRETATION AND DISCUSSION

We have interpreted all of these results as follows:

Below about 750°C, the phase $Ce_2(Co_{0.5}Fe_{0.5})_{17}$ becomes unstable and decomposes on cooling by the eutectoid reaction

$$Ce_2(Co_{0.5}Fe_{0.5})_{17} \longrightarrow a\ Co_{0.37}Fe_{0.63} + b\ Ce_2(Co_{0.74}Fe_{0.26})_7$$

with a ~ b as determined by metallographic inspection. This reaction can be suppressed by rapid cooling so that $Ce_2(Co_{0.5}Fe_{0.5})_{17}$ can be retained in metastable form at room temperature.

Between 851°C and 879°C, the $Ce_2(Co_{0.74}Fe_{0.26})_7$ melts by peritectic reaction on heating

$$Ce_2(Co_{0.74}Fe_{0.26})_7 \longrightarrow \text{Liquid} + Ce_2(Co_{1-y}F_y)_{17}\ (y < 0.5)$$

and the liquid phase immediately reacts with the $Co_{0.37}Fe_{0.63}$ alloy by the inverse peritectic reaction

$$\text{Liquid} + Co_{0.37}Fe_{0.63} \longrightarrow Ce_2(Co_{1-z}Fe_z)_{17} \quad (z > 0.5)$$

With increasing time and temperature above the temperature of these reactions, $z \longrightarrow x \longleftarrow y$ and $Ce_2(Co_{0.5}Fe_{0.5})_{17}$ is restabilized.

This series of events readily explains the magnetic and thermal events observed by TMA and DTA, respectively.

(1) Reheating the metastable $Ce_2(Co_{0.5}Fe_{0.5})_{17}$ above approximately 500°C provides sufficient thermal energy to initiate the eutectoid decomposition reaction. The disappearance of the T_c of the 2-17 phase on cycling reflects the degree to which the decomposition reaction has gone to completion.

(2) The weak, second order-type reaction observed between 661°C and 673°C by DTA but not by TMA is apparently the order-disorder reaction of the phase Co-Fe present in the $Co_{0.37}Fe_{0.63}$ alloy, see Elliott[3].

(3) The intense thermal event observed in the range of 851°C - 879°C by DTA are the peritectic and simultaneous inverse peritectic reactions described above. The intense magnetic event observed at the same temperature is not a Curie transition but rather results from the disappearance of the Co-Fe alloy by the inverse peritectic reaction while it is still below its magnetic ordering temperature.

(4) The relatively intense TMA event observed between 672°C and 765°C on cooling marks the onset of the eutectoid decomposition of the re-formed $Ce_2(Co, Fe)_{17}$ phase or phases. What the TMA detects is the reappearance of a Co-Fe phase which is already below its Curie temperature. Since this is a relatively sluggish eutectoid reaction, it is not a strong DTA event.

(5) Finally, the re-emergence of the T_c of the 2-17 phase after heating above 980°C or so indicates that the eutectoid reaction has not gone to completion during cooling.

The instability of the $Ce_2(Co_{1-x}Fe_x)_{17}$ phases in the range $0.4 \leq x \leq 0.8$ apparently results from the large mechanical strain induced by the forced ferromagnetic alignment of Fe atoms occupying sensitive positions in the 2-17 structure. The source of this strain has been discussed in detail elsewhere[4]. The phases are stable at high temperatures because they are well above their Curie temperatures. The similarity of the TMA results obtained for the iron-rich $Sm_2(Co, Fe)_{17}$ and $MM_2(Co, Fe)_{17}$ alloys with the $Ce_2(Co, Fe)_{17}$ phases suggest they also become unstable when cooled below their magnetic ordering temperatures.

It is somewhat surprising that the Ce-rich decomposition product of the $Ce_2(Co_{0.5}Fe_{0.5})_{17}$ phase is a $Ce_2(Co, Fe)_7$ phase. One might have expected a $Ce(Co, Fe)_2$ phase to form since both the terminal phases, $CeCo_2$ and $CeFe_2$ exist, or perhaps a $Ce(Co, Fe)_3$ phase, since $CeCo_3$ exists and other RFe_3 phases are known, although not $CeFe_3$[5]. Evidentally, $Ce_2(Co_{0.74}Fe_{0.26})_7$ represents the maximum extent of Ce_2Co_7 into the ternary Ce-Co-Fe system at 850°C, the temperature at which $Ce_2(Co_{0.5}Fe_{0.5})_{17}$ was decomposed.

REFERENCES

1. A. E. Ray and K. J. Strnat, "Research and Development of Rare Earth-Transition Metal Alloys as Permanent-Magnet Materials," AFML-TR-72-99, April, 1972, pp. 10-18.

2. A. E. Ray and K. J. Strnat, "Research and Development of Rare Earth-Transition Metal Alloys as Permanent-Magnet Materials," AFML-TR-72-210, October, 1971, p. 20.

3. R. P. Elliott, "Constitution of Binary Alloys, First Supplement." McGraw-Hill, New York, 1965, pp. 319-320.

4. A. E. Ray and R. S. Harmer, Proceedings of the 9th Rare Earth Research Conference, Blacksburg, Virginia, Vol. 1, 1971, pp. 368-378. See also ref. 2, Appendix, p. 108.

5. A. E. Ray, Proceedings of the 7th Rare Earth Research Conference, Coronado, California, Vol. II, 1968, pp. 473-484.

SECTION III

THE NEODYMIUM-COBALT PHASE DIAGRAM*

A. INTRODUCTION

The Ce-Co, Pr-Co, and Nd-Co alloy systems were previously studied by Ray and Hoffer[1] and tentative but incomplete phase diagrams were proposed. During the present contractual effort, previously unreported phases were found to exist in each of these binary alloy systems. It is suspected that some of these, namely the R_5Co_{19} phases, may play significant roles in the achievement of high coercive forces in sintered RCo_5 magnets. In view of the importance of reliable phase diagrams as guides for alloy preparation, heat treatment, and the understanding and control of the magnetic behavior of these alloys, we are revising and completing these three binary phase diagrams. The revised Pr-Co system was reported in AFML-TR-71-210. The revised Nd-Co is reported below. We hope to commence the revision of the Ce-Co system within the next few months. Dr. F. H. Spedding of the Ames Laboratory at Iowa State University has graciously agreed to prepare and supply us with high purity cerium metal for this latter project.

B. MATERIALS AND ALLOY PREPARATION

The neodymium and cobalt metals used for the alloy preparation were obtained from the Lunex Company and from the African Metals Corporation, respectively. Chemical analyses of the metals, provided by the suppliers, are given in Table I.

The alloys were prepared by arc melting the component elemental metals in a purified argon-helium atmosphere. The alloys were melted, then inverted and remelted several times to enhance mixing. Weight losses during melting seldom exceeded 0.1%. The alloy compositions were assumed

* Ray, Biermann, Harmer, Geis

TABLE I

Analyses of Neodymium and Cobalt Metals

Used for Alloy Preparation

(Impurities in ppm)

Element	Nd	Element	Nd	Element	Cobalt (Lot Co-3799)
Si	---	La	---	S	10
Mn	1*	Ce	---	C	70
Mg	---	Pr	50*	Fe	30
Al	---	Sm	5*	Zn	30
Ta	10*	Eu	---	Cu	20
Pb	10*	Gd	1*	Ni	430
Ca	200*	Tb	50*	Si	20
Be	10*	Dy	5*	Mn	5
B	50*	Hb	50*	P	3
Nb	---	Er	100*	Pb	4
Na	5*	Tm	5*		
Li	---	Yb	---		
Zn	50*	Lu	5*		
Zr	20*	Leco O_2	540		
Cd	5*	Kjeldahl N_2	27		

* No persistent line was found The value reported is the detection limit for the element.

--- Indicates interference and no estimate could be made.

to be the nominal compositions, not including an additional 2 wt.% Nd which was added to each alloy to correct for the impurity content, primarily oxygen, in the neodymium. The value of 2 wt.% Nd was the amount of excess Nd required to produce metallographically single phase alloys of the stoichiometric compounds, Nd_3Co and $NdCo_2$.

The alloys containing from 0 to 25 at.% Co were examined in the as-arc melted condition, while alloys containing more than 25 at.% Co were wrapped in Ta foil and homogenized in vacuum for three to seven days at temperatures 25°C to 100°C below the lowest melting phase known to be present in the particular alloy.

C. EXPERIMENTAL PROCEDURES

The alloys were examined by metallographic, x-ray diffraction, electron microprobe, and differential thermal analyses. For metallographic examination, the alloys containing up to 50 at.% Co were etched with 0.1% nital while the more cobalt-rich alloys were etched with 1.0% nital. X-ray diffraction patterns were obtained with a G. E. XRD-6 diffractometer and Type 700 detector system, using CrK_α radiation. Lattice constants were determined by the methods of Vogel and Kempter[2] with the aid of an RCA Spectra 70/40 computer. Nickel powder was used as an internal standard to correct for zero degree 2θ errors. Microprobe analysis was done with a MAC Model 5 Electron Microprobe X-Ray Analyzer. The stoichiometric intermetallic phases Nd_3Co and $NdCo_2$ were used as standards. The differential thermal analysis equipment employed has been described in detail elsewhere[3]. Tantalum crucibles and thermocouple sheaths were used for alloys containing from 0 to 25 at.% Co, while high density alumina crucibles and sheaths were used for alloys containing more than 25 at.% Co. Thermocouples employed were W/26 Re vs. W/3 Re obtained from Englehard Industries.

D. RESULTS

The proposed phase diagram for the neodymium cobalt phase diagram is shown in Figure 1. The invariant reactions observed in the system are discussed below.

Nd - The neodymium metal obtained from the Lunex Company was observed to melt at 1017 ±2°C and undergo the $\alpha \rightleftharpoons \beta$ transformation at 859 ±3°C. These values compare favorably with those of Johnson, et al.[4] who report 1019 ±2°C for the melting point and 869 ±2°C for the $\alpha \rightleftharpoons \beta$ transformation, respectively. The solubility of cobalt in neodymium was not determined but appears to be very small.

Eutectic I - A eutectic reaction between α-Nd and Nd_3Co occurs at 625 ±3°C and 20.0 ±0.5 at.% Co. The microstructure of an as-cast 20 at.% Co alloy is shown in Figure 2.

Nd_3Co - The intermetallic phase Nd_3Co melts congurently at 646 ±2°C. The R_3Co phases have been previously described by Buschow[5] to be orthorhombic with the Fe_3C - type crystal structure. They report the lattice constants for Nd_3Co to be a = 7.107 Å, b = 9.750 Å, and c = 6.386 Å. We measured slightly larger values for Nd_3Co, namely a = 7.125 ±2 Å, b = 9.764 ±3 Å, and c = 6.409 ±3 Å. The microstructure of an as-cast 25 at.% Co alloy is shown in Figure 3.

Nd_xCo - An intermetallic phase, Nd_xCo, containing 29.0 ±0.5 at.% Co forms by peritectic reaction at 596 ±2°C between Nd_3Co and liquid (30.5 ±0.5 at.% Co.) Electron microprobe analysis, using Nd_3Co as a standard, shows Nd_xCo to contain 28.96 ±0.22 at.% Co. The crystal structure of Nd_xCo is undetermined, but its diffraction pattern is similar to a phase found at 29.5 ±0.5 at.% Co in the Pr-Co alloy system. The d-spacings of the two phases are compared in Table II. Both of these are probably similar in structure to the phase containing about 30 at.% Co found by

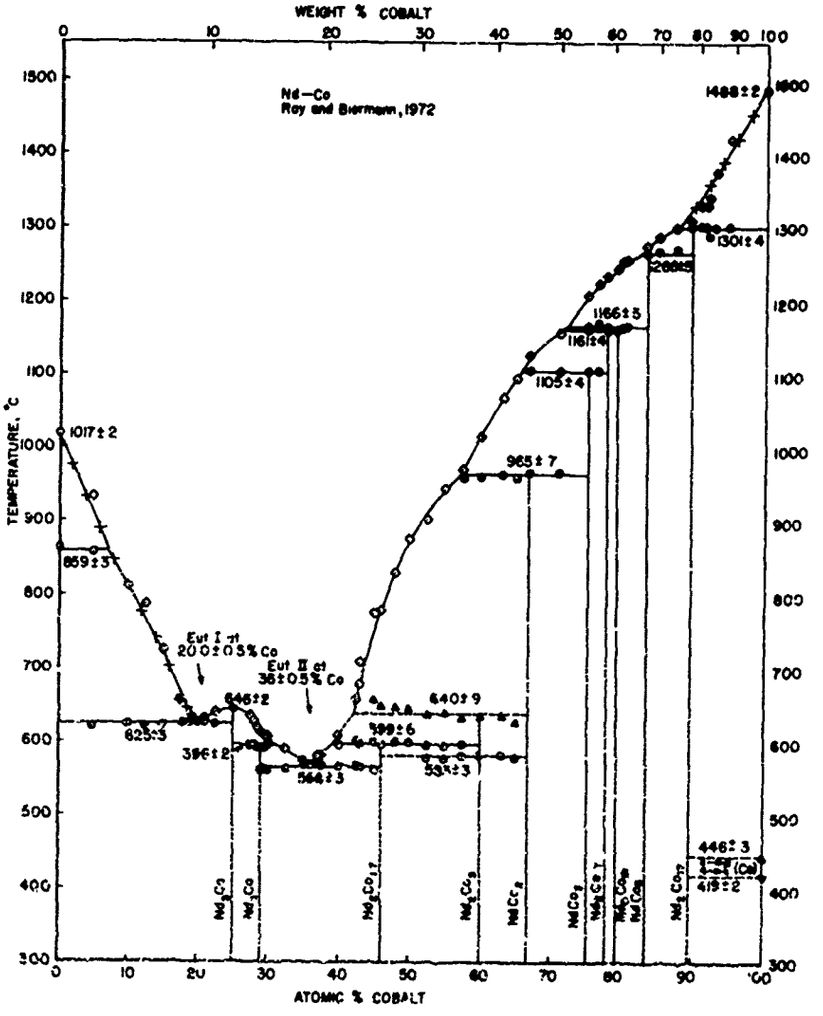

Figure 1. Phase diagram for the neodymium-cobalt alloy system.

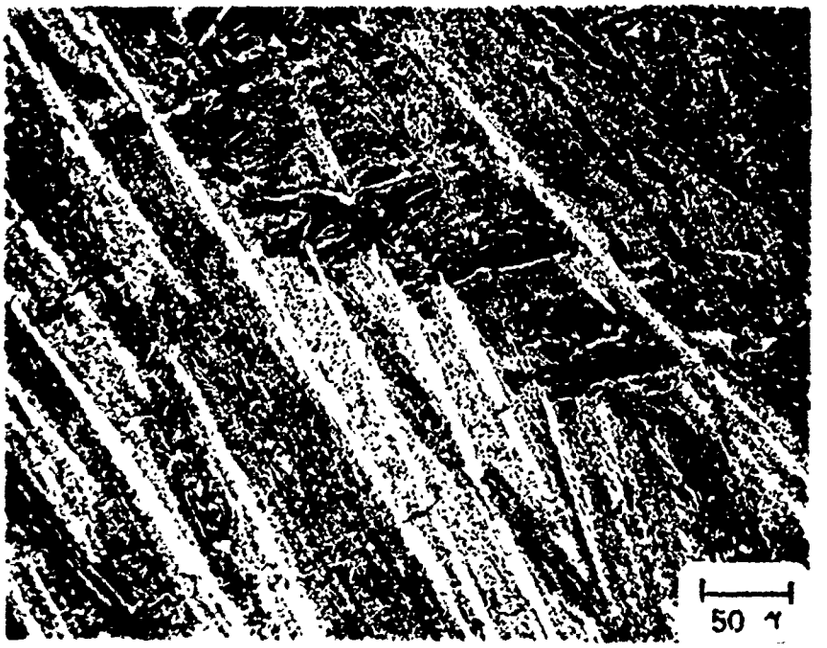

Figure 2. Nd-20 at.% Co alloy, as-cast, Eutectic I.

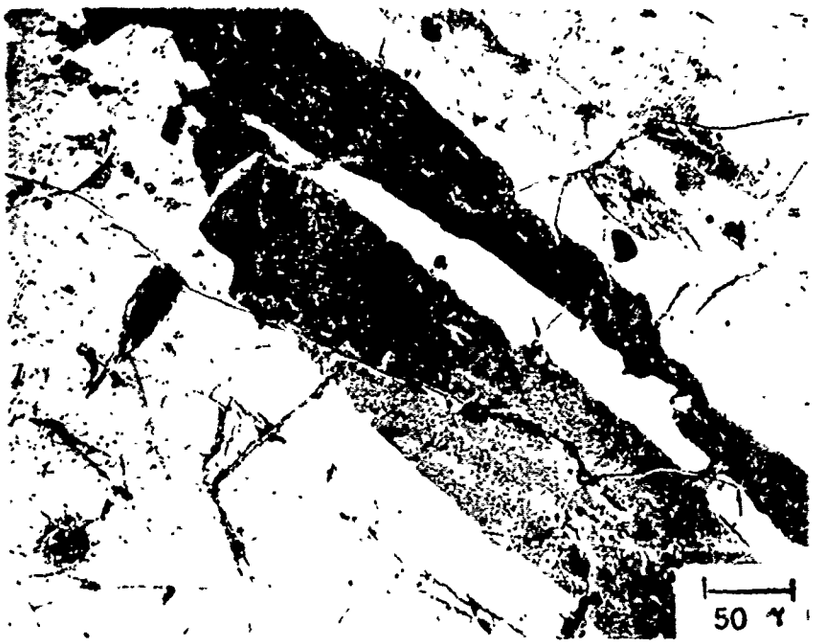

Figure 3. Nd-25 at.% Co alloy, as-cast, Nd_3Co.

TABLE II

Comparison of X-Ray Diffraction Patterns for Pr_xCo and Nd_xCo (~29 at.% Co)

Pr_xCo		Nd_xCo	
Int	d, Å	Int	d, Å
W	3.483	VW	3.478
W	3.255	W	3.250
W	3.180		-----
M	3.110	M	3.112
W	2.993		-----
S	2.944	S	2.951
		S	2.934
S	2.820	M	2.820
M	2.741	M	2.738
M	2.622	M	2.615
M	2.596	M	2.594
M	2.548	M	2.544
W	2.453	W	2.448
VW	2.398	W	2.388
	-----	W	2.370
VW	2.345	VW	2.342
W	2.291	W	2.285
W	2.253	VW	2.249
M	2.224	M	2.223
W	2.160	VW	2.157
W	1.960	W	1.955
W	1.919	VW	1.918
W	1.781	W	1.775
W	1.760	VW	1.751
W	1.729	W	1.722
W	1.714	M	1.712
	-----	W	1.671
	-----	W	1.640
	-----	W	1.595
	-----	W	1.581

Buschow and Van der Goot[6] and assigned the formula Sm_9Co_4. The microstructure of a 30.0 at.% Co alloy homogenized at 550°C is shown in Figure 4.

Eutectic II - A eutectic reaction occurs at 566±3°C and 36±0.5 at.% Co between Nd_xCo and $Nd_2Co_{1.7}$. The microstructure of an as-cast 36 at.% Co alloy is shown in Figure 5.

$Nd_2Co_{1.7}$ - The intermetallic phase $Nd_2Co_{1.7}$ forms by peritectic reaction at 599±6°C and 46±0.5 at.% Co between Nd_2Co_3 and liquid (39±1 at.% Co). $Nd_2Co_{1.7}$ is hexagonal with a = 3.795±2 Å and c = 4.09±2 Å. This phase is isostructural with $Pr_2Co_{1.7}$ and has been described elsewhere[7]. The microstructure of a 46 at.% Co alloy homogenized at 540°C is shown in Figure 6.

Nd_2Co_3 - The intermetallic phase Nd_2Co_3 forms by peritectic reaction between $NdCo_2$ and liquid. The equilibrium temperature of the Nd_2Co_3 peritectic reaction is uncertain. Statistically, the event observed on DTA heating cycles is centered at 640 ±9°C, and the peritectic reaction is tentatively indicated by a dashed isotherm at this temperature. A corresponding cooling event which could be definitely associated with the formation of Nd_2Co_3 was not observed. Apparently, Nd_2Co_3 is not readily nucleated from the liquid plus $NdCo_2$ phase field and forms simultaneously with $Nd_2Co_{1.7}$ on cooling. At 45 at.% Co, a weak, diffuse, endothermic event peaking at 659°C is observed by DTA on heating. The intensity of this heating event increases and becomes less diffuse with increasing cobalt content up to 60 at.% Co. The temperature at which the event is observed, however, gradually decreases with increasing cobalt content. It is observed at 647°C at 50 at.% Co, 636°C at 60 at.% Co, and 627°C at 65 at.% Co. Figure 7 shows the nearly single phase microstructure of a 60 at.% Co alloy which has been annealed at 625°C for 500 hours.

A second thermal event, apparently associated with a crystal structure change in Nd_2Co_3, is observed at 583±3°C for alloys containing

Figure 4. Nd-30 at.% Co alloy, annealed 72 hrs at 575°C, Nd_xCo (gray) plus a small amount of $Nd_2Co_{1.7}$ (white).

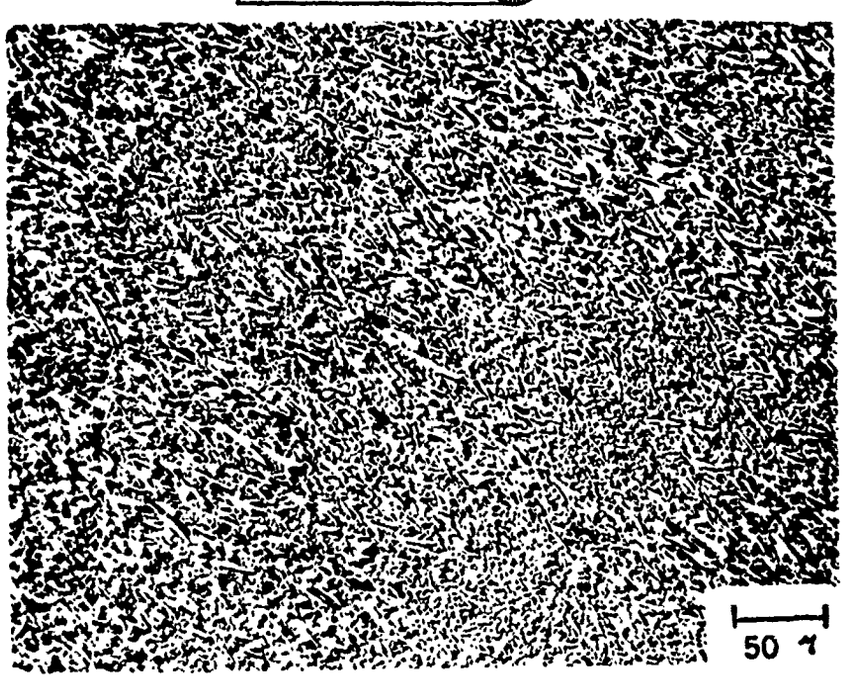

Figure 5. Nd-36 at.% Co alloy, as-cast, Eutectic II.

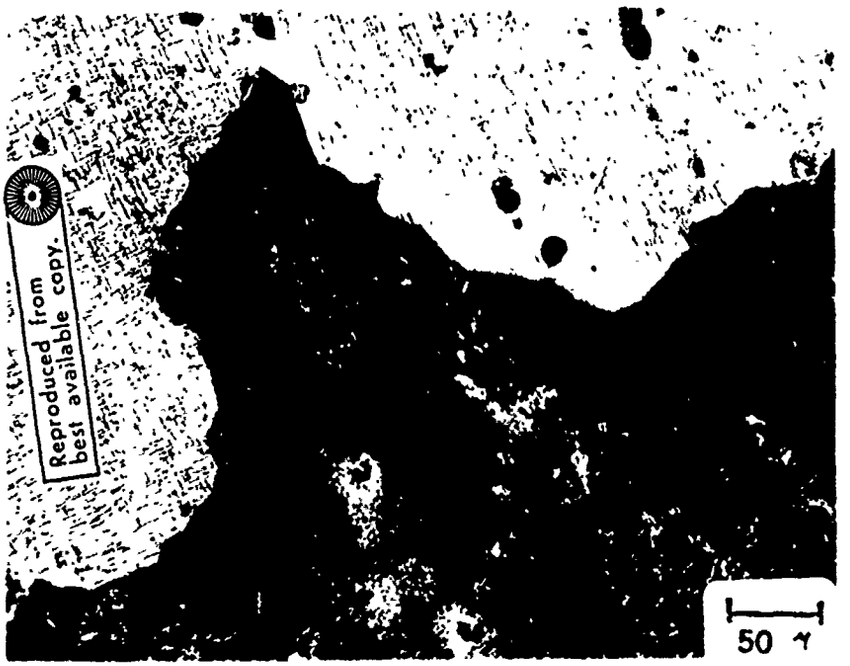

Figure 6. Nd-46 at.% Co alloy, annealed 168 hrs at 570°C, $Nd_2Co_{1.7}$ plus a small amount of Eutectic II (dark spheroidal phase).

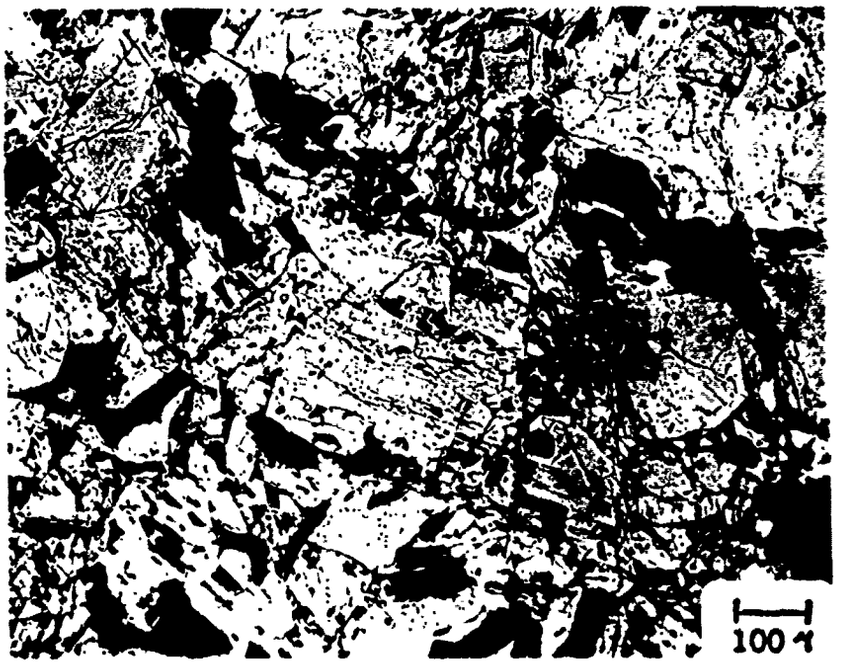

Figure 7. Nd-60 at.% Co alloy, annealed 500 hrs at 625°C, Nd_2Co_3 plus a small amount of $Nd_2Co_{1.7}$ (dark gray phase). The black areas are voids.

between 52.5 and 65 at.% Co. The high temperature form of Nd_2Co_3, if one exists, is unknown. At room temperature, Nd_2Co_3 is orthorhombic with a = 10.006±2 Å, b = 4.963±2 Å, and c = 7.569±4 Å. Nd_2Co_3 appears to be isostructural with the phase La_2Co_3 reported by Buschow and Velge[8]. Electron microprobe analysis, using $NdCo_2$ as a standard, shows the actual composition of Nd_2Co_3 to be 60.8±0.3 at.% Co.

$NdCo_2$ - The intermetallic phase $NdCo_2$ (66.7 at.% Co) forms by peritectic reaction at 965±7°C between $NdCo_3$ and liquid (57±1 at.% Co). $NdCo_2$ has a cubic $MgCu_2$-type structure with a = 7.297±2 Å. The microstructure of a 66.7 at.% Co alloy homogenized at 925°C is shown in Figure 8.

$NdCo_3$ - The intermetallic phase $NdCo_3$ (75 at.% Co) forms by peritectic reaction at 1105±4°C between Nd_2Co_7 and liquid (65.5±1.0 at.% Co). $NdCo_3$ has a rhombohedral $PuNi_3$-type structure with a = 5.070±1 Å and c = 24.75±1 Å. The microstructure of a 75 at.% Co alloy homogenized at 950°C is shown in Figure 9.

Nd_2Co_7 - The intermetallic phase Nd_2Co_7 (77.8 at.% Co) forms by peritectic reaction at 1161±4°C between Nd_5Co_{19} and liquid (71.5±1.0 at.% Co). Nd_2Co_7 has the hexagonal Ce_2Ni_7-type with a = 5.062±2 Å and c = 24.45±1 Å. The microstructure of a 77.8 at.% Co alloy homogenized at 1120°C is shown in Figure 10.

Nd_5Co_{19} - The intermetallic phase Nd_5Co_{19} (79.2 at.% Co) forms by peritectic reaction at 1166±5°C between $NdCo_5$ and liquid (72±1 at.% Co). Nd_5Co_{19} apparently has both rhombohedral and hexagonal modifications with nearly identical a axes and $c_{rh} \approx 3/2\ c_{hex}$. The rhombohedral form is strongly dominant with a = 5.054±2 Å and c = 48.66±3 Å. Nd_5Co_{19} is isostructural with Pr_5Co_{19}[7]. The microstructures of alloys containing 79.2 and 79.5 at.% Co, homogenized near 1100°C are shown in Figures 11 and 12, respectively.

Figure 8. Nd-66.7 at.% Co alloy, annealed 96 hrs at 925°C, $NdCo_2$ plus a small amount of $NdCo_3$ (light phase).

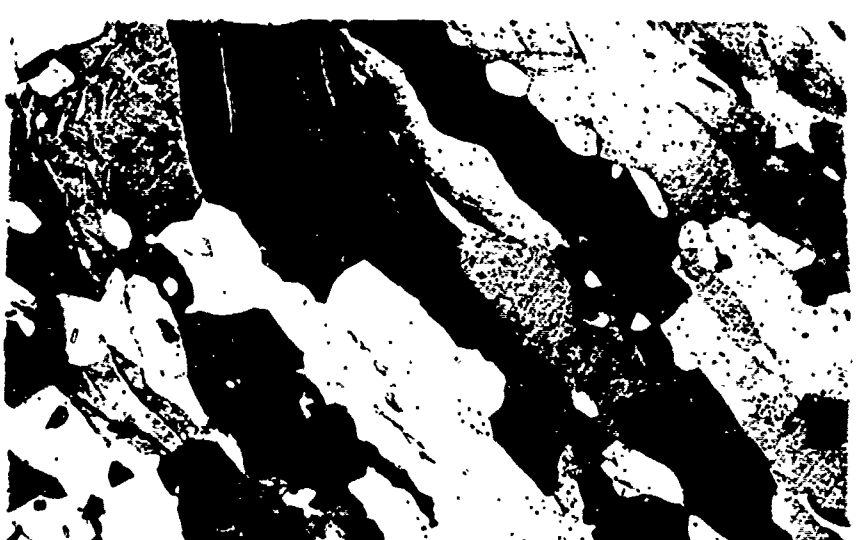

Figure 9. Nd-75 at.% Co alloy, annealed 48 hrs at 950°C. Primarily $NdCo_3$, the small, spheroidal grains are Nd_2Co_7.

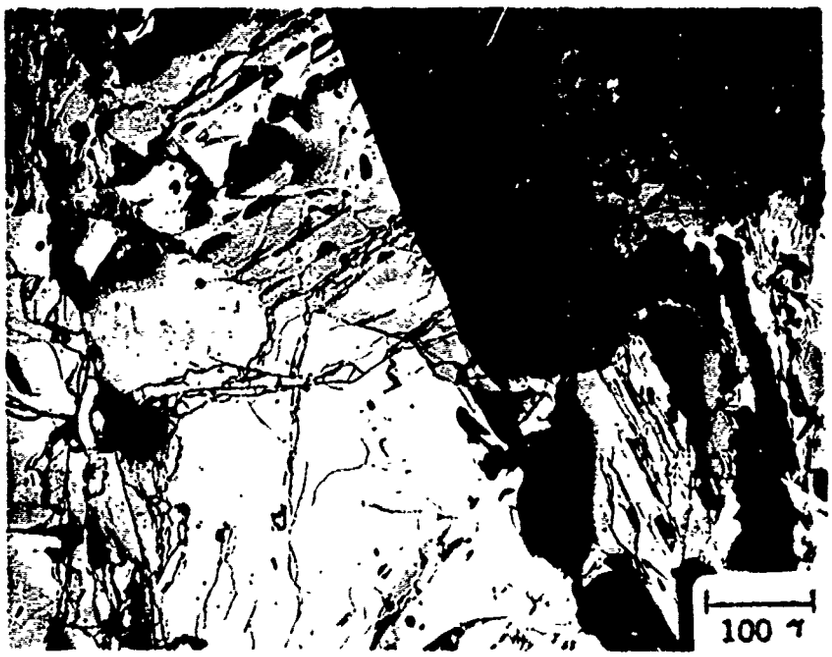

Figure 10. Nd-77.8 at.% Co alloy, annealed 48 hrs at 1120°C, Nd_2Co_7. The black areas are voids.

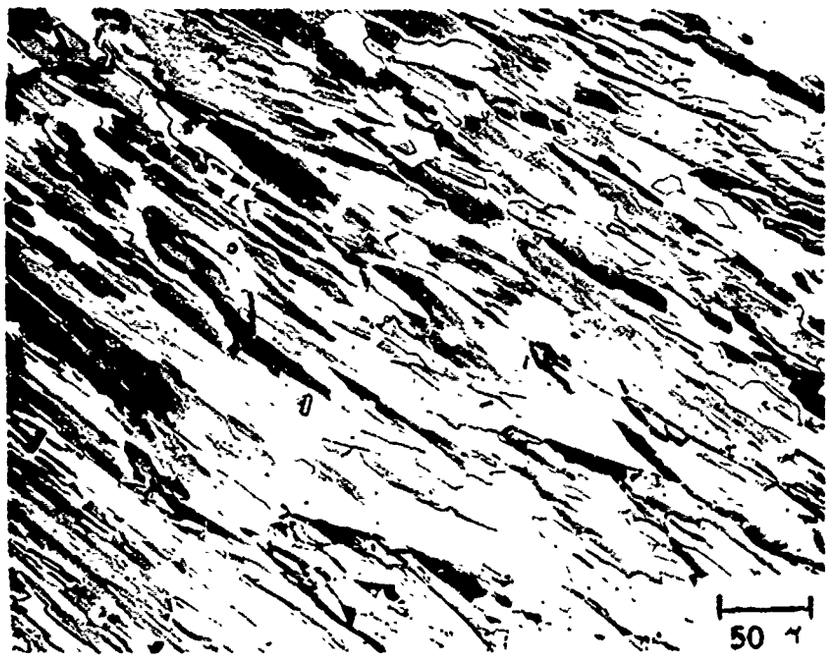

Figure 11. Nd-79.2 at.% Co alloy, annealed 48 hrs at 1120°C, Nd_5Co_{19}.

$NdCo_5$ - The intermetallic phase $NdCo_5$ (88.3 at.% Co) forms by peritectic reaction at 1266±5°C between Nd_2Co_{17} and liquid (82±1 at.% Co). $NdCo_5$ has the $CaZn_5$-type structure with a = 5.028±1 Å and c = 3.977±2 Å at the stoichiometric composition. A small range of solubility extending to the Co-rich side of $PrCo_5$ may occur since we observe a = 5.027±1 Å and c = 3.981±2 Å in the $PrCo_5$ + Pr_2Co_{17} phase field for alloys homogenized at 1100°C. The microstructure of an alloy containing 83.3 at.% Co homogenized at 1200°C is shown in Figure 13.

Nd_2Co_{17} - The intermetallic phase Nd_2Co_{17} forms by peritectic reaction at 1301±4°C between β-Co and liquid (87.5±1.0 at.% Co). Nd_2Co_{17} has the rhombohedral Th_2Zn_{17}-type structure with a = 8.426±2 Å and c = 12.425±2 Å. The microstructure of an alloy containing 89.5 at.% Co homogenized at 1150°C is shown in Figure 14.

Co - The cobalt metal obtained from African Metals was observed to melt at 1488±2°C, to transform from α (cubic) to β (hexagonal) on heating at 446±3°C, and from β to α at 419±2°C. The values are in reasonable agreement with previously reported values of 1495°C and 417°C for the melting and transformation temperatures, respectively[9].

Calculation of the Liquidus Boundary * - The liquidus boundaries for the terminal phases of the Nd-Co systems were calculated with the aid of the following assumptions:

1. The terminal solid solubility region is of negligible width.
2. The free energy of the liquid phase can be described by the quasi-chemical theory of a regular solution.
3. The difference between the heat capacities of the solid and liquid phases is zero.

---

* Dr. J. E. Davison of the School of Engineering, University of Dayton, developed the analytical expressions and computer programs, as well as carried out the actual computations for this portion of the system. His assistance is gratefully acknowledged.

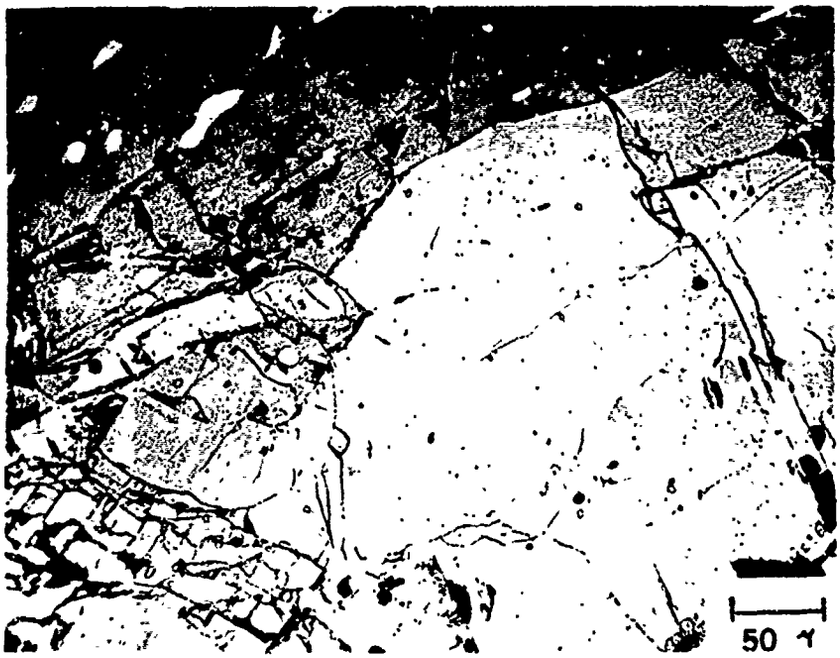

Figure 12. Nd-79.5 at.% Co alloy, annealed 24 hrs at 1050°C plus 72 hrs at 1100°C. Nd_5Co_{19} plus some $NdCo_5$ (the light, spheroidal phase).

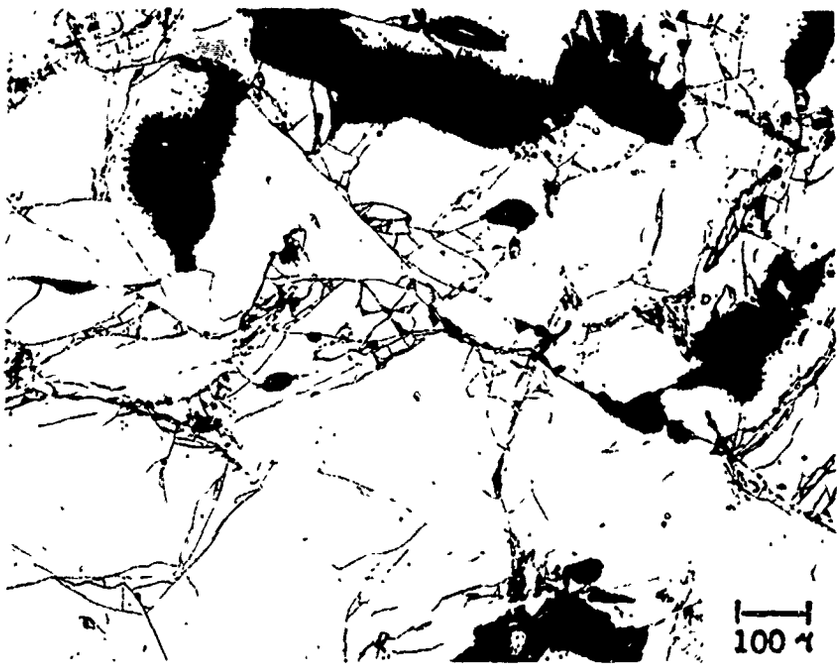

Figure 13. Nd-83.3 at.% Co alloy, annealed 48 hrs at 1200°C, $NdCo_5$.

Figure 14. Nd-89.5 at.% Co alloy, annealed 72 hrs at 1150°C, Nd_2Co_{17}.

With these assumptions it can be shown that the analytical representation of the neodymium liquidus phase boundary is given by the relation,

$$RT \ln N_{Nd,L} + \Omega_{Nd\text{-}Co}(1 - N_{Nd,L})^2 = \Delta H_{f,Nd}(1 - \frac{T}{T_{Nd}}) \ .$$

The quantities, R, $\Delta H_{f,Nd}$, and T_{Nd}, are, respectively, the universal gas constant, the enthalpy of fusion of pure neodymium, and the melting temperature of pure neodymium, the quantity, $\Omega_{Nd\text{-}Co}$, is the pairwise energy parameter of the quasi-chemical theory, and the quantity, $N_{Nd,L}$, represents the mole fraction of the liquidus boundary at the temperature, T. The parameter, $\Omega_{Nd\text{-}Co}$, was determined from the above equation by combining the required thermodynamic data of pure elemental neodymium with an experimental measurement of the temperature and composition of that liquidus boundary. The liquidus boundary is then calculated over an extended temperature and composition range with the parameter fixed at this value. The cobalt liquidus phase boundary was calculated in a similar manner.

Curie Temperatures - Curie temperatures obtained by differential thermal analysis (DTA) are less precise than those obtained by thermal magnetic analysis (TMA). Nevertheless, thermal events corresponding to Curie temperatures were observed for the cobalt-rich Nd-Co phases with T_c's above room temperature. These are given in Figure 15 plotted against composition. An almost linear relationship between T_c and composition is noted.

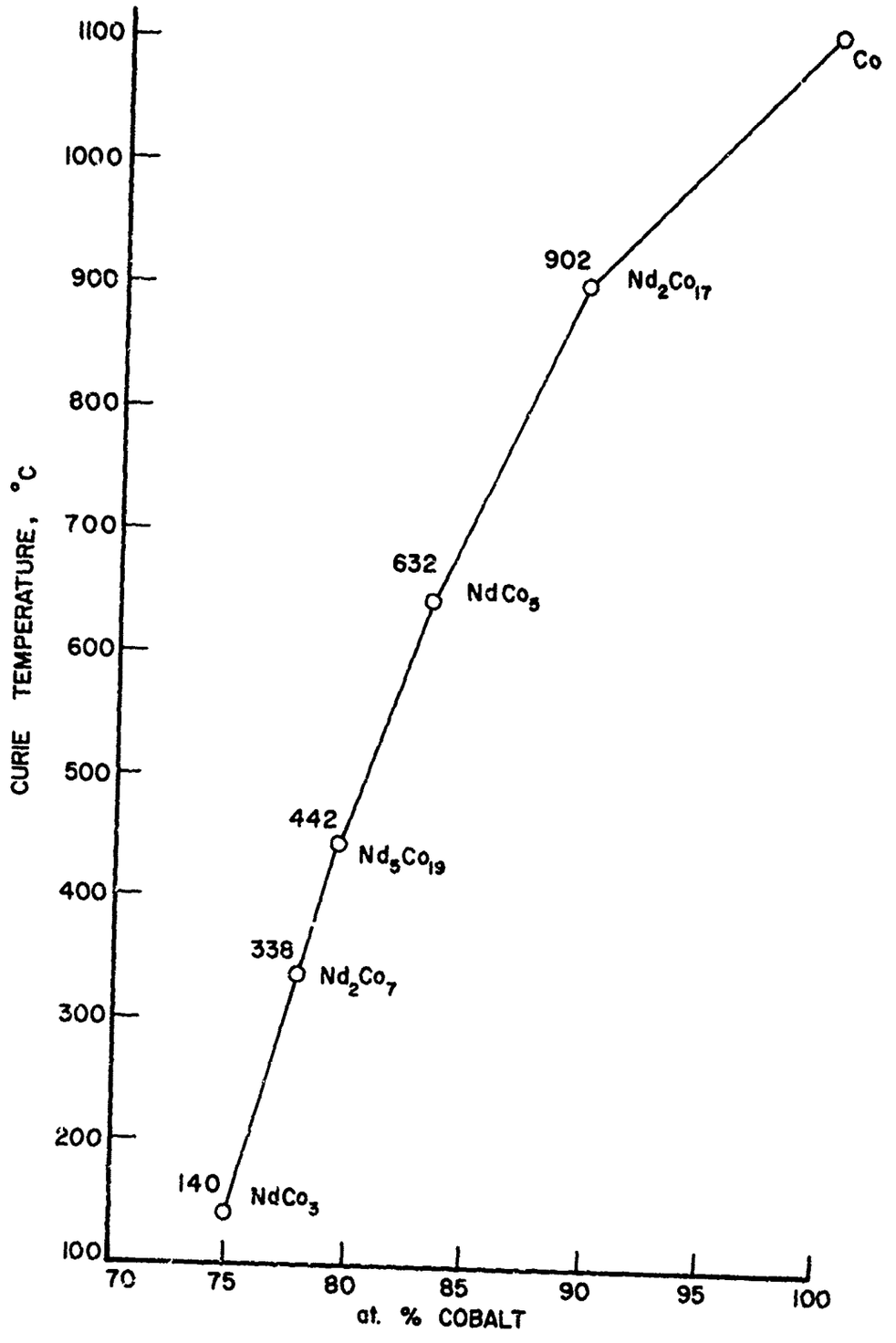

Figure 15. Plot of Curie temperatures measured by DTA versus composition for the Co-rich Nd-Co phases.

REFERENCES

1. A. E. Ray and G. I. Hoffer, Proceedings of the 8th Rare Earth Research Conference, Reno, Nevada, Vol. II, 1970, p. 529.

2. R. E. Vogel and C. P. Kempter, Acta Cryst., Vol. 14, 1961, p. 1130.

3. A. E. Ray and K. J. Strnat, "Research and Development of Rare Earth-Transition Metal Alloys as Permanent-Magnet Materials," AFML-TR-71-53, Wright-Patterson Air Force Base, Ohio, March, 1971, p. 21.

4. R. G. Johnson, D. E. Hudson, W. C. Caldwell, F. H. Spedding, ar. W. R. Savage, J. Chem. Phys., Vol 25, 1956, p. 917.

5. K. H. J. Buschow, Philips Research Reports, Vol. 26, 1971, p. 49.

6. K. H. J. Buschow and A. S. Van der Goot, J. Less-Common Metals, Vol. 17, 1969, p. 249.

7. J. Schweizer, "Research on Rare Earth-Cobalt Alloys and Compounds," AFML-TR-72-82, Wright-Patterson Air Force Base, Ohio, May, 1972.

8. K. H. J. Buschow and W. A. J. J. Velge, J. Less Common Metals, Vol. 13, 1967, p. 11.

9. F. R. Morral, Metals Handbook, 8th Edition, American Society for Metals, Metals Park, Ohio, Vol. 1, p. 1201.

SECTION IV

HIGH MAGNETIC COERCIVITY OF NEODYMIUM- AND DIDYMIUM-COBALT ALLOYS SINTERED WITH Pr AND Sm ADDITIONS*

A. INTRODUCTION

Several rare earth-cobalt intermetallic compounds of the type RCo_5 are excellent permanent magnet materials because of their high, positive uniaxial magnetic crystal anisotropy[1, 2]. $SmCo_5$ is the best example. Its first-order anisotropy constant at 300°K is $K_1 \approx 11 \times 10^7$ erg/cm^3, and fine powders of $SmCo_5$ produced by mechanical grinding can have extremely high intrinsic coercive forces, ${}_M H_c$ = 10 to 20 kOe. However, $NdCo_5$ is an exception among the RCo_5. It has single-easy-axis symmetry at room temperature[3], but the anisotropy constant is relatively small ($K_1 \approx 6 \times 10^6$) [4] decreases on cooling and changes sign near 270°K. Micron-size particles of $NdCo_5$ have a coercive force of less than 200 Oe. It had therefore been concluded that $NdCo_5$ could not be used for magnets, although its other properties such as the high saturation ($B_s \approx 14,000$ G), Curie point (T_c = 913°K) and the relatively great abundance and potentially low cost of neodymium would make it attractive for this application[1, 2].

The preferred method for producing rare earth-cobalt magnets is now liquid-phase sintering with an excess of R over the RCo_5 composition[5]. From previous sintering experiments with $PrCo_5$ we developed the hypothesis that the coercive force of sintered bodies may be due to domain-wall pinning in second-phase regions or "shells" which are contiguous with the RCo_5 grains[6]. If this idea is correct, then the coercivity should be determined more by the properties of the shell than by those of the core material. It should then be possible to surround $NdCo_5$ grains with a high

* J. B. Y. Tsui, K. J. Strnat and J. Schweizer (present address: Centre d'Etudes Nucleaires, Grenoble, France)

anisotropy phase which can effectively pin walls, e.g., an $(R,Nd)_2Co_7$ alloy where R is Sm or Pr, and thus to force the composite to have the high coercive force of the latter.

This section reports the results of some preliminary experiments which were conducted to test this possibility. In addition to $NdCo_5$, we also used as the "base metal" the alloy $DiCo_5$, where Di stands for "didymium". This is a commercial rare earth product* which is principally a mixture of neodymium with praseodymium and is less expensive than either pure Nd or Pr. $DiCo_5$ has some of the undesirable magnetic properties of $NdCo_5$ -- primarily a relatively low and strongly temperature dependent anisotropy -- but to a lesser degree.

B. EXPERIMENTAL PROCEDURE

Four different alloys were used in these sintering experiments. All of them were prepared by arc-melting in a water-cooled copper hearth under argon following previously described procedures. The RCo_5 base-metal buttons were homogenized at 1100°C for 48 hours; the two alloys used as liquid-phase sintering additives were ground in the as-cast condition. Metallography and x-ray diffraction showed the $DiCo_5$ alloy to be essentially single-phase while the alloy designated as $NdCo_5$ contained approximately 35% of Nd_2Co_{17} as a second phase.** (Nd_2Co_{17} has a low crystal anisotropy of the easy-basal-plane type at room temperature and is thus also a poor fine-particle permanent magnet material.)[7] The sintering aids were the same two which had been used in previous experiments with $PrCo_5$[6,8]. One was an alloy of approximately 70 weight % Pr and 30 w/o Co, the other had 60 w/o Sm and 40 w/o Co.

---

* The didymium metal used was supplied by the Ronson Metals Corporation. The "typical analysis" given is 70-75%Nd, 17-19% Pr, 0.3-0.5% Ce, 8-12% other rare earths.

** The Nd-Co alloy and the Pr-Co alloy used as the sintering additive were both prepared several years ago at the US Bureau of Mines in Reno, Nevada, by an electrowinning process. Both were remelted in the arc furnace.

The powders for the sintering experiments were prepared by hand grinding in a mortar to <105 μm particle size followed by grinding in an attritor-type ball mill under toluene. The two base metals were ground for 5 minutes, the sintering aid 70 Pr/30 Co for 60 minutes, and the alloy 60 Sm/40 Co for 30 minutes. The alloy powders were dried, blended, aligned in a magnetic field of 36 kOe and compacted into small bricks at 125 kpsi[8]. These were sintered in vacuum under the conditions stated below and then allowed to cool fairly rapidly by withdrawing the quartz bulbs from the furnace. (The average cooling rate between the sintering temperature and 900°C was approximately 1000°C per minute.)

C. EXPERIMENTAL RESULTS

Coercivity of Ground Powders

To establish reference values, the two base-metal alloys were also mortar ground and the powder separated into size fractions by sifting and with the aid of a centrifugal particle classifier. All samples were found to have quite low coercive forces. The results are summarized in Table I. The attritor-miller powders had similarly low coercivity. The values measured on compacts in the green state before sintering were $_{M}H_{c}$ = 190 Oe for $NdCo_5$ and 130 Oe for $DiCo_5$. These measurements were done with a DC hysteresigraph in peak fields of 10 kOe; a peak magnetizing field of 25 kOe was used in measuring the sintered samples.

TABLE I

COERCIVE FORCE OF MORTAR-GROUND POWDERS

Particle Size (μm)	53-74	37-53	< 37	< 20
$NdCo_5$ ($_{M}H_{c}$)	55	50	90	350
$DiCo_5$ (Oe)	all < 20 Oe			

$NdCo_5$ Sintered with a 70 Weight % Pr/30 Weight % Co Additive

Samples were prepared in the range from 20 to 50 weight % of the sintering aid. This corresponds to total cobalt contents of the resulting magnets between 63 and 51% (calculated using 71% as the Co content of the base alloy). In this experiment, all samples were sintered at 1140°C for a period of 30 minutes. The results are shown in Figure 1. It can be seen that a maximum intrinsic coercive force of 4000 Oe was obtained, which corresponds to a more than twenty-fold increase over the coercivity of the powder. However, hysteresis loop shapes were poor and the remanence values low.

The average particle size of the $NdCo_5$ was between 5 and 10 μm, that of the sintering additive between 3 and 5 μm, as judged by inspection of scanning electron micrographs of the powders.

$DiCo_5$ Sintered with an Additive of 70 Weight % Pr/30 Weight % Co

The powders used in this experiment had approximately the same particle sizes as those used before. Again, a series of samples with varying amounts of sintering aid between 20 and 50% was prepared. The samples were sintered at 1140°C for 30 minutes. The maximum coercive force for the sample with 40% additive was $_{M}H_{c}$ = 3850 Oe. Three duplicate samples with 20, 30 and 40% sintering aid were stored in a high vacuum for 6 months before they were sintered under exactly the same conditions as before. Their coercivities were considerably higher, with a maximum value of 8820 Oe for the 40% sample. This corresponds to an increase of 68 times over the green sample. The reason for this different behavior is not understood, but it is assumed that it is attributable to the thorough out-gassing and complete removal of all traces of the grinding liquid.

Next, a series of experiments was conducted in which a sample containing 20 weight % additive was heated repeatedly for successive 30-minute intervals, starting at 1040°C and increasing the sintering

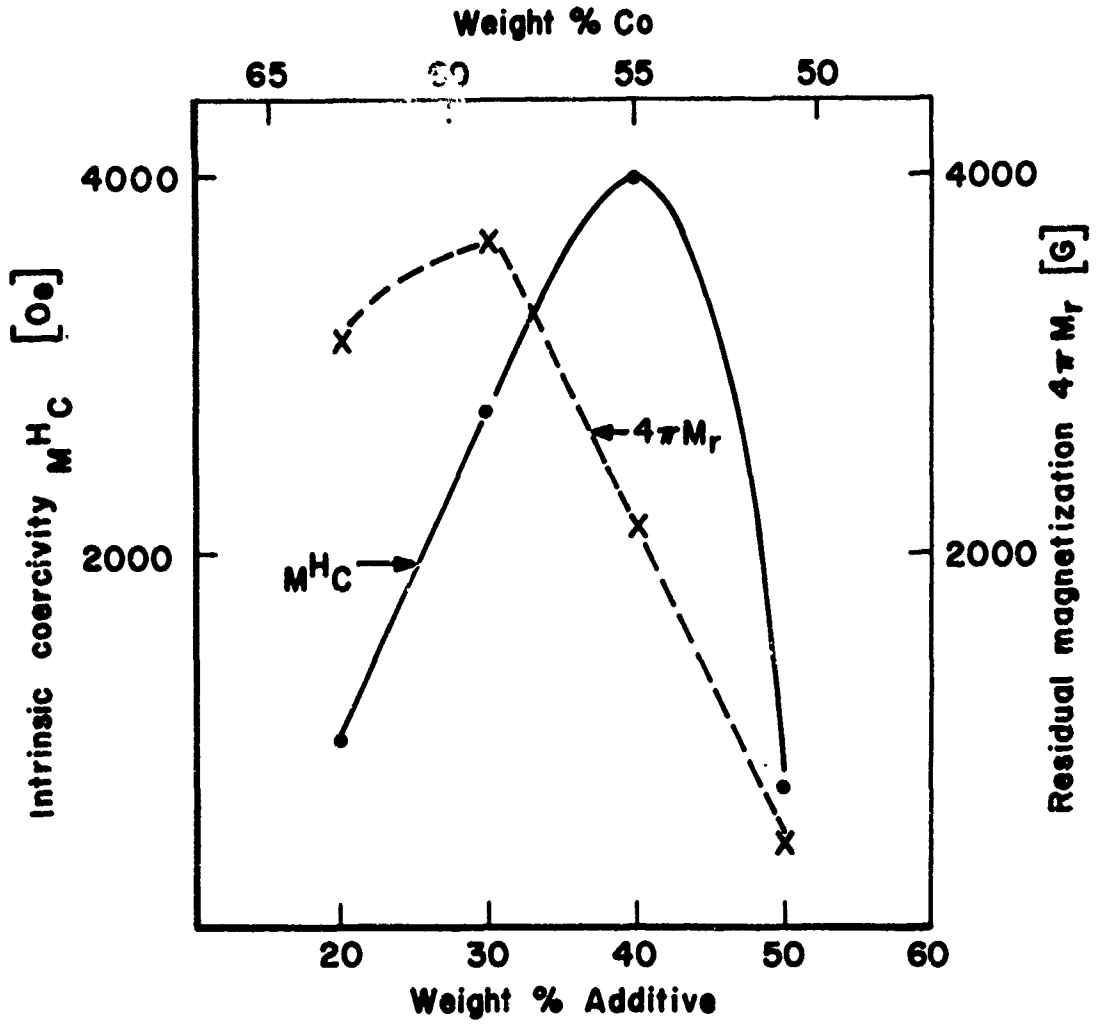

Figure 1. Sintering of $NdCo_5$ with a 70% Pr/30% Co additive. All samples vacuum sintered for 30 minutes at 1140°C.

temperature in six steps to a maximum of 1160°C. The results are shown by the solid line in Figure 2. The temperature dependence of the intrinsic coercive force resembles closely that found in similar experiments with $PrCo_5$ [6], but the general level of coercivity is much lower here. The same sample was then taken through a second cycle of heating steps in which it was again held for 30 minutes at each temperature level, beginning at 1020°C and proceeding to 1140°. The results are represented by the dashed curve which shows the same general shape as the solid line but reaches a maximum of only 800 Oe. Finally, two new samples of identical composition were prepared and sintered at 1100°C and 1140°C, respectively. The coercive forces, indicated by the open circles in Figure 2, agree well with the minimum and maximum values found in the first experiment.

$DiCo_5$ Sintered with an Additive of 60 Weight % Sm and 40 Weight % Co

The attritor-milled $DiCo_5$ was the same as used before. The 60 Sm/40 Co additive was ground to ~ 5 μ average particle size. First, the influence of the ratio of base metal to additive was studied. Six samples covering a range of 10 to 40 % additive were prepared. They were sintered at 1160°C for 30 minutes. The results are shown in Figure 3. A maximum of $_MH_c$ = 5140 Oe was obtained for 25 w/o additive, but it appears from the graph that the curve may have its peak at a slightly lower sintering-aid content.

Next, a sample of 22.5 w/o additive was sintered repeatedly at increasing temperatures as mentioned above. The results are shown in Figure 4 (solid line). The curve has three peaks: the highest peak occurred at 1040°C with $_MH_c$ = 7700 Oe, the following two peaks at higher temperature are lower in height. In the second heating cycle of the same sample, two of the peaks disappeared and, again, the level of coercive force is generally much lower. To check the repeatability of these results, two new samples of the same composition were sintered at 1100°C and 1140°C. Their coercive forces are shown as open circles and again match quite well the

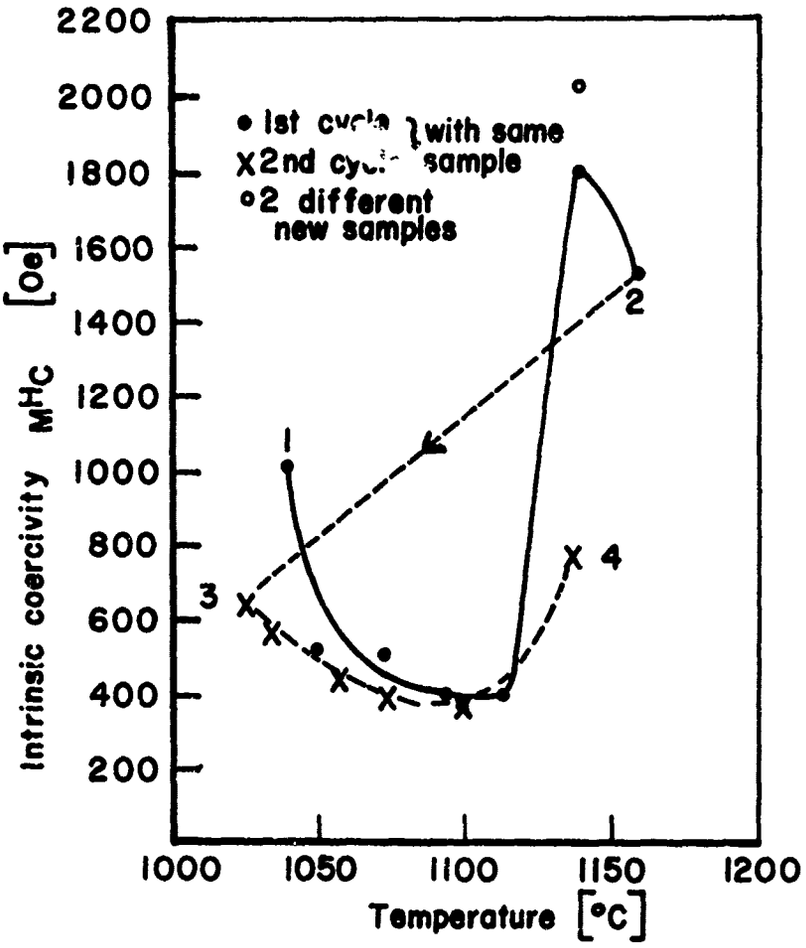

Figure 2. Sintering of $DiCo_5$ with a 70% Pr/30% Co additive. All samples contained 80% $DiCo_5$ and 20% of the additive. One sample was heated repeatedly in two cycles indicated by the numbers 1, 2, 3, 4 on the curves.

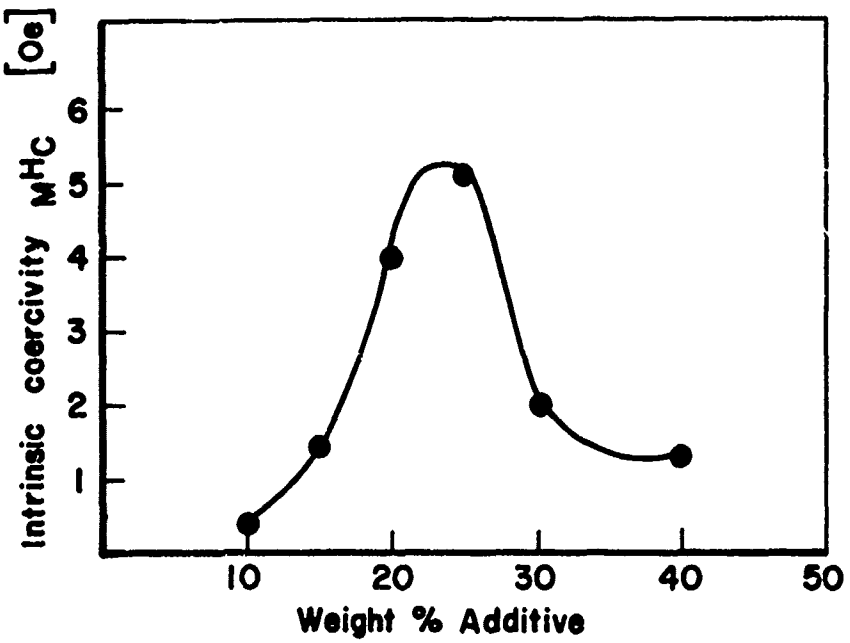

Figure 3. $DiCo_5$ sintered with a 60% Sm/40% Co additive at 1160°C for 30 minutes.

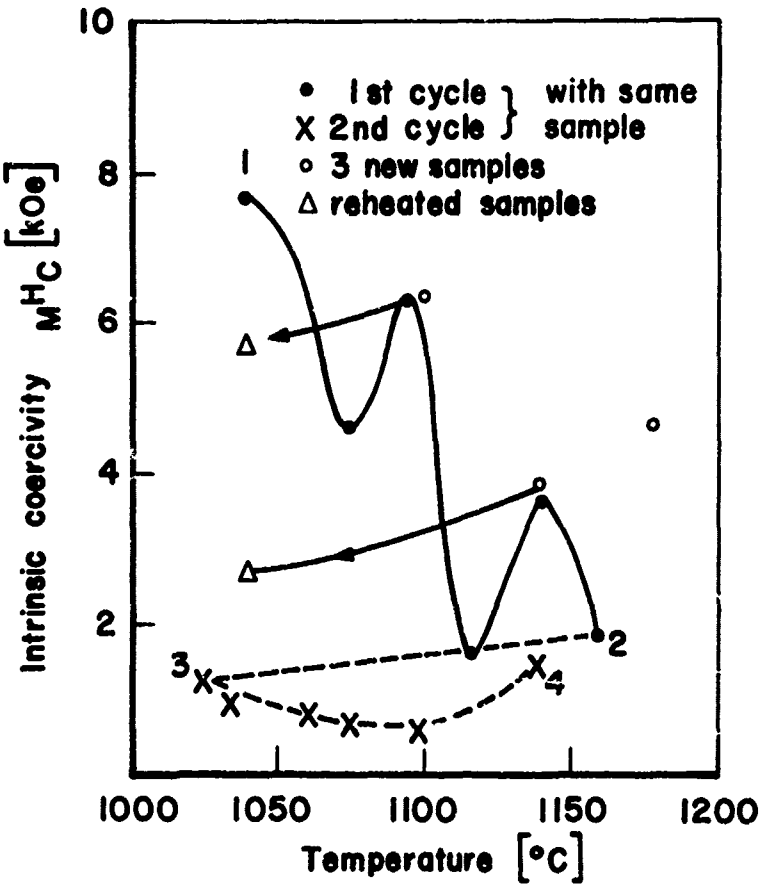

Figure 4. Sintering of $DiCo_5$ with a 60% Sm/40% Co additive. All samples contained 77.5% $DiCo_5$ and 22.5% additive. One sample was heated repeatedly in two cycles indicated by the numbers1, 2, 3, 4 on the curves.

corresponding values on the solid line. These two samples were then reheated at 1040°C for 30 minutes and this treatment lowered their $_{M}H_{c}$ as shown by the triangles. A third, newly-prepared sample was sintered at 1180°C. It had a higher coercive force than the samples sintered between 1020° and 1060°C. Due to the limitations of the furnace, sintering temperatures above 1180°C could not be used.

Next, the dependence $_{M}H_{c}$ upon the sintering time was studied for samples sintered at the apparent optimum temperature of 1040°C. One sample having 22.5 w/o Sm-Co, another of 17.5 w/o Sm-Co were prepared. Both were sintered simultaneously at 1040°C for 15 minutes, cooled to room temperature and measured. Then these samples were sintered again for an additional period of time and so on. The coercivity versus the cumulative total sintering time is shown in Figure 5. The peak coercive force value obtained was 10,280 Oe for the sample with 17.5 w/o Sm-Co after 60 minutes. This constitutes an increase of almost 80 times over the green-sample value.

D. CONCLUSIONS

While ground powders of $NdCo_5$ and $DiCo_5$ have low coercive forces of a few 100 Oe at the most, liquid-phase sintering of these alloys with a Pr-rich or, especially, a Sm-rich sintering aid is capable of producing magnets with quite useful intrinsic coercive forces up to 10 kOe. This surprising fact may be attributable to the formation of epitaxial shells of Sm or Pr-rich compounds having high anisotropy field and wall-pinning strength. However, it is also possible that the added rare earth diffuses uniformly through the base-metal grains and raises the bulk anisotropy of the latter. Further experiments designed to clarify the mechanism of this great enhancement of the coercivity are now in progress.

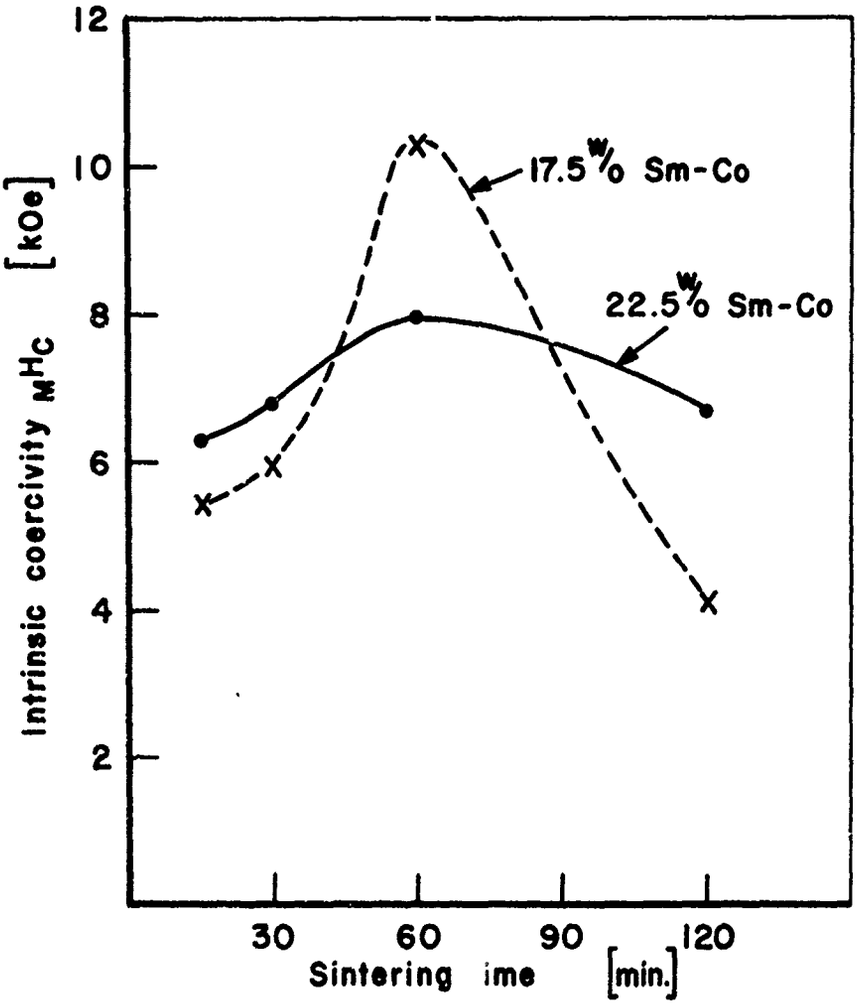

Figure 5. Sintering of $DiCo_5$ with a 60% Sm/40% Co additive. Samples vacuum sintered at 1040°C.

REFERENCES

1. K. J. Strnat, IEEE Trans. Magnetics, MAG-4,(1970), p. 182.

2. J. J. Becker, J. Appl. Physics, 41, (1970), p. 1055.

3. H. Bartholin, B. van Laar, R. Lemaire and J. Schweizer, J. Phys. Chem. Solids, 27, (1966), p. 1287.

4. E. Tatsumoto, T. Okamoto, H. Fujii and C. Inoue, J. de Physique, 32, (1971), C1-550.

5. M. G. Benz and D. L. Martin, AIP Conference Proceedings, No. 5, Part 2, p. 1082, Am. Inst. Physics, 1972.

6. J. Schweizer, K. J. Strnat, and J. B. Y. Tsui, IEEE Trans. Magentics, MAG-7, (1971), p. 429.

7. H. Mildrum, J. Schweizer and J. B. Y. Tsui, University of Dayton, unpublished information. See also Ref. 1.

8. K. J. Strnat, J. B. Y. Tsui and J. Schweizer, Proceedings of the 9th Rare Earth Research Conference, Vol. I, p. 252, Blacksburg, Virginia, October, 1971.